Published by Avanti Publishers

The Global Environmental Engineers

ISSN (online): 2410-3624

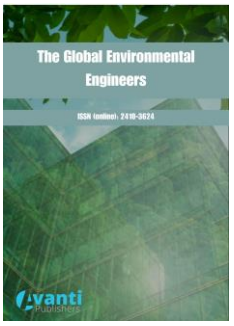

Recent Progress in Using Peroxymonosulfate for the Treatment of Organic Wastewater – A Brief Review

Nannan Wang[1,2,*], Ye Yang[1], Kai Wang[3], Xu Liu[1], Zishan Hou[1], Xiangyu Liu[1], Siquan Zou[1] and Zaixing Li[1,2,*]

[1]*Department of Environmental Engineering, Beijing Institute of Petrochemical Technology, Beijing 102617, PR China*

[2]*Wastewater Nitrogen Integrated Treatment Technology Innovation Center of Hebei Province, Shijiazhuang 050000, PR China*

[3]*Department of Energy Engineering, Beijing Institute of Petrochemical Technology, Beijing 102617, PR China*

ARTICLE INFO

Article Type: Review Article

Academic Editor: Shuangquan Yao

Keywords:
Catalysts
Activation
Reactive oxygen species
Degradation of organic contaminants

Timeline:
Received: June 05, 2025
Accepted: August 02, 2025
Published: August 20, 2025

Citation: Nannan W, Ye Y, Kai W, Xu L, Zishan H, Xiangyu L, Siquan Z, Zaixing L. Recent progress in using peroxymonosulfate for the treatment of organic wastewater – A brief review. Glob Environ Eng. 2025; 12: 37-60.

DOI: https://doi.org/10.15377/2410-3624.2025.12.4

ABSTRACT

In recent years, peroxymonosulfate advanced oxidation processes (PMS-AOPs) have become an attractive method for the treatment of refractory organic wastewater, relying on their ability to generate highly oxidizing active species (SO_4·-, ·OH, and $^1O_2$, etc.). In this review, the characteristics of PMS-AOPs are firstly introduced, followed by a systematic introduction of peroxymonosulfate (PMS) activation methods, including energy-assisted activation, metal-based material activation, carbon-based material activation, and composite system activation. Subsequently, the effects of critical parameters (wastewater pH, reaction temperature, PMS dosage, catalyst loading, inorganic ions and natural organic matter, and reaction time) on the performance of PMS-AOPs were discussed. Furthermore, the working mechanisms of PMS in PMS-AOPs were proposed, and finally, potential research directions in the near future were suggested. This review provides fundamental analysis and discussion of PMS-AOPs in the treatment of refractory organic wastewater.

*Corresponding Authors
Email: wnn_flying@163.com and li_zaixing@163.com
Tel: +(86) 13704517275

1. Introduction

With the acceleration of global industrialization and urbanization, large amounts of wastewater containing refractory organic pollutants are discharged into the water environment [1]. The pollutants in wastewater are often complex in structure, highly toxic, high bioaccumulation, and persistent in the environment, posing a serious threat to human health and the balance of ecosystems [2]. Traditional physical methods (such as adsorption, filtration, and membrane separation) and biological treatment methods are often costly and ineffective (exhibiting low removal efficiency and/or incomplete mineralization) for treating such refractory organic pollutants [3-5]. Therefore, it is urgent to develop new wastewater treatment technologies that are low-cost, high-efficiency and environmentally friendly.

In recent years, peroxymonosulfate advanced oxidation processes (PMS-AOPs) have emerged as a promising solution for degrading refractory organic pollutants due to their ability to generate highly reactive oxygen species (ROS) such as $SO_4^{\cdot-}$, ·OH and $^1O_2$ [6]. Numerous reviews have explored the activation methods and proposed radical/non-radical mechanisms of PMS-AOPs, however, these studies narrowly focus on specific activators or mechanisms, they lack systematic analysis of operational parameters and compatibility with actual water matrices [7-10].

Our review first introduces the characteristics of PMS-AOPs, and then systematically summarizes peroxymonosulfate (PMS) activation methods, including energy-assisted activation (thermal, photocatalytic, electrochemical and plasma activation), metal-based material activation (homogeneous and heterogeneous system activation), carbon-based material activation, and composite system activation. Subsequently, this review discusses the influence of key factors such as reaction conditions (pH, temperature), oxidation system parameters (PMS dosage and catalyst loading), and water matrix components (inorganic ions, natural organic matter) on PMS-AOPs performance. Finally, this paper discusses the working mechanism of PMS and proposes future research directions for PMS-AOPs. The objective of this review is to provide a fundamental analysis of PMS-AOPs for treating refractory organic wastewater; to bridge the knowledge gap between laboratory research and practical application; and to guide future research towards scalable, sustainable organic wastewater treatment solutions.

2. Characteristics of PMS-AOPs

PMS and peroxydisulfate (PDS) are typical oxidants in the persulfate advanced oxidation processes (AOPs) [11]. They exhibit distinct properties and structures, as detailed in Table **1** and Fig. (**1**). PDS has a symmetrical structure and is more stable; in contrast, PMS has an asymmetrical structure and is relatively easier to activate by activators [12, 13]. Therefore, many scholars have chosen PMS for their research in recent years.

Table 1: Critical physicochemical properties of PMS and PDS.

	Molecular Formula	Oxidation-Reduction Potential (V)	O-O bond Moment	O-O Bond Energy (kJ/mol)	Solubility (g/L)
PMS	HSO5-	1.82	1.460	140.2 – 213.3	>250
PDS	S2O82-	2.01	1.497	140.2	556

As a new type of oxidant, PMS has attracted much attention in AOPs due to its high efficiency and environmental friendliness [14, 15]. Compared with traditional Fenton technology, which relies on the strong oxidation capacity of ·OH, the $SO_4^{\cdot-}$ generated by PMS activation have a higher oxidation-reduction potential (2.5 – 3.1 V) and can efficiently break the chemical bonds of complex organic pollutants. It exhibits excellent performance in the degradation of refractory organic compounds such as antibiotics and persistent organic pollutants [6, 16]. In addition, the PMS system has broken through the limitations of traditional Fenton technology, which relies on an acidic environment (pH 2 – 4). It can maintain its activity under neutral to alkaline conditions, significantly reducing the energy consumption and operating costs of pH adjustment in practical applications [17]. From a reaction kinetics perspective, the half-life of $SO_4^{\cdot-}$ (30 – 40 μs) is extended by 1 – 2 orders of magnitude

compared to ·OH (<1 μs). This characteristic enables it to diffuse more easily to the pollutant interface in heterogeneous systems, thereby enhancing mass transfer efficiency and degradation rates [18]. Additionally, PMS is stored in solid powder form with high stability. Its activation methods are diverse, including thermal energy, light radiation, transition metal catalysis, and interaction with carbon-based material interfaces, providing flexible technical adaptability for different water quality conditions and application scenarios.

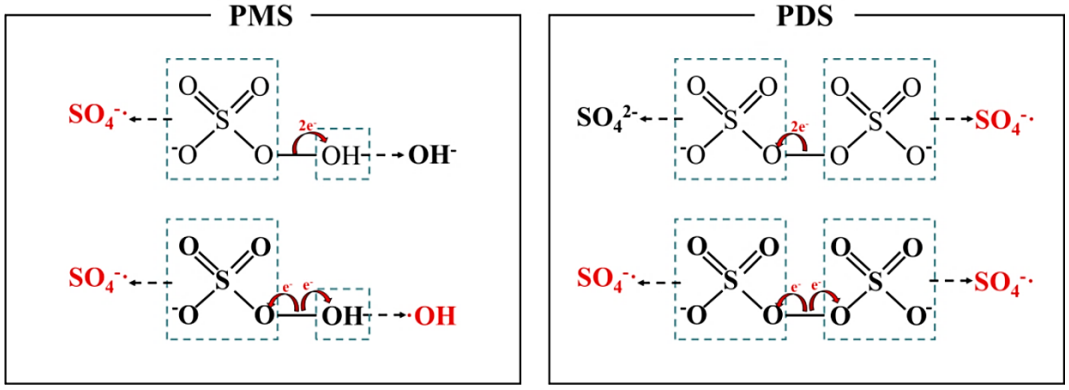

Figure 1: Comparison of the molecular structures and activation processes of PMS and PDS.

The activation of PMS is a critical step in realizing its oxidative potential. Different activation methods trigger PMS decomposition through energy transfer, electron transfer, or surface interactions, thereby producing ROS. The ROS produced after PMS activation are diverse, mainly including $^1O_2$, $O_2^{\bullet-}$, $SO_4^{\cdot-}$ and ·OH. The active substances that play a dominant role in different systems are generally different.

3. Activation Method for PMS

3.1. Energy-assisted Activation

3.1.1. Thermal Activation

The core mechanism of thermal activation lies in the increase in molecular thermal motion caused by heat energy, which promotes the breaking of O-O bonds in PMS, generating highly active $SO_4^{\cdot-}$ and ·OH [19, 20]. The reaction pathway is shown in Eq. (1). When the reaction temperature was increased from 40°C to 80°C, the removal efficiency of tetracycline by PMS within 90 minutes increased from 75.7% to 95.6% [21]. Thermal activation of PMS can also enhance the selectivity of the system for pollutant degradation. When real coking wastewater was treated with 60°C/PMS, the biodegradability index (BOD_5/COD) of the wastewater was significantly increased from the initial 0.21 to 0.4 after 60 minutes of reaction. Additionally, as shown in Fig. (**2**), the removal rates of two typical nitrogen-containing heterocyclic compounds (quinoline and indole) in the wastewater were selectively degraded by 45% and 85%, respectively [22]. Traditional direct heating can directly increase the temperature of the reaction system through heat transfer, but it typically requires a long heating time and is limited by the heat transfer processes of conduction and convection from the outside to the inside. This results in low thermal efficiency and significant heat loss.

$$HSO_5^- \xrightarrow{\Delta} SO_4^{\cdot-} + \cdot OH \quad (1)$$

As a high-frequency electromagnetic wave, microwave (MW) energy can be absorbed by polar molecules or ions within a substance and directly converted into heat energy at the molecular level through a dielectric heating mechanism, thereby heating the reaction system [23]. MW-assisted thermal activation PMS significantly promotes the removal of thermally stable organic pollutants. As shown in Fig. (**2**), the MW/PMS system achieved a 97.9% removal rate of atrazine within 30 minutes, which is 3.5 times that of the traditional heating/PMS system [24]. This inward-outward heating method avoids the heat transfer limitations of traditional external heating and significantly improves the heating rate and efficiency. However, due to its high energy consumption, MW heating is currently still in the laboratory stage and is difficult to apply in practice.

Figure 2: Schematic diagram of the selective degradation of nitrogenous heterocyclic compounds in phenol-rich coking wastewater by thermal-activated PMS [22].

Thermal activation can effectively break the O-O bond of PMS to produce ROS. However, excessive temperatures (>80°C) may cause free radicals to self-quench or trigger side reactions, thereby reducing the removal efficiency of target pollutants [25]. Therefore, optimizing the temperature range (usually 30 – 80°C) is key to the engineering application of thermal activation technology. In actual wastewater treatment, thermal activation PMS technology has the advantages of no catalyst addition and simple operation, but continuous heating results in high equipment operating costs. Thermal activation can be coupled with other technologies.

3.1.2. Photocatalytic Activation

Photocatalytic activation of PMS generally utilizes the light absorption properties of semiconductor materials (such as TiO_2 and $BiVO_4$) to generate electron-hole pairs (e^--h^+) under illumination [26, 27]. Conduction band electrons (e^-) directly activate PMS to generate $SO_4^{\bullet-}$, while valence band holes (h^+) can oxidize water or pollutants. The reaction process is shown in Eqs. (2), (3) [28].

$$HSO_5^- + e^- \rightarrow SO_4^{\bullet-} + \cdot OH \quad (2)$$

$$H_2O + h^+ \rightarrow \cdot OH \quad (3)$$

The light sources commonly used in photocatalytic PMS activation technologies are mainly ultraviolet (UV) and visible light [29]. High-energy UV light has a higher activation efficiency for PMS, as its photon energy is sufficient to directly break the O-O bond in PMS, thereby efficiently generating a variety of ROS [30]. In UV/PMS systems, pollutant degradation generally occurs through multiple pathways, including direct oxidation (UV photolysis and PMS oxidation) and radical oxidation ($SO_4^{\bullet-}$ and ·OH) [31]. Compared to PMS oxidation alone and direct UV photolysis, the UV/PMS system achieved a degradation rate of >99% for initial concentrations of 60 μM Cu(II)-EDTA within 10 minutes [32]. UV activation is an environmentally friendly technology that does not require additional chemical reagents. However, this method has significant limitations in practical applications, primarily because the UV component of sunlight is extremely low (typically less than 5%), resulting in limited available natural light energy [28].

However, the photon energy of visible light is relatively low and typically insufficient to directly break the O-O bonds in PMS. Therefore, visible light responsive catalysts are often required to achieve visible light activation of PMS [33]. A study prepared a PTCDA/MIL-88A(Fe) photosensitive catalyst to activate PMS, achieving a 98.4% removal efficiency of the herbicide 2,4-dichlorophenoxyacetic acid under 300 W LED visible light conditions within 10 minutes [34]. Additionally, modifying catalysts through element doping or constructing heterojunctions can efficiently promote charge separation and transfer, and effectively expand their photo response range to the visible light region [35-37]. A study used hexagonal boron nitride (h-BN) as an electron sink to construct a Cu_2O@BN heterojunction catalyst for photocatalytic activation of PMS to degrade bisphenol A. The degradation efficiency was 3.8 times higher than the Cu_2O/PMS/Light system [38]. Graphitic carbon nitride (g-C_3N_4) exhibits excellent photo responsive properties [39, 40]. Elemental doping at its interstitial sites significantly enhances its

photocatalytic performance [41]. The co-doping of sulfur (S) and chlorine (Cl) elements effectively regulates the electronic structure of the catalyst surface, thereby significantly enhancing the light absorption capacity and photocatalytic activation performance of g-C_3N_4 [42]. As shown in Fig. (**3**), while the SCl-CN photocatalyst efficiently activates PMS to produce more $SO_4^{\cdot-}$ and ·OH, the electron transfer efficiency is also greatly increased. The reaction rate constants for pollutant degradation are 3.5 times, 13.4 times, and 14.7 times higher than CN, S-CN, and Cl-CN, respectively [43].

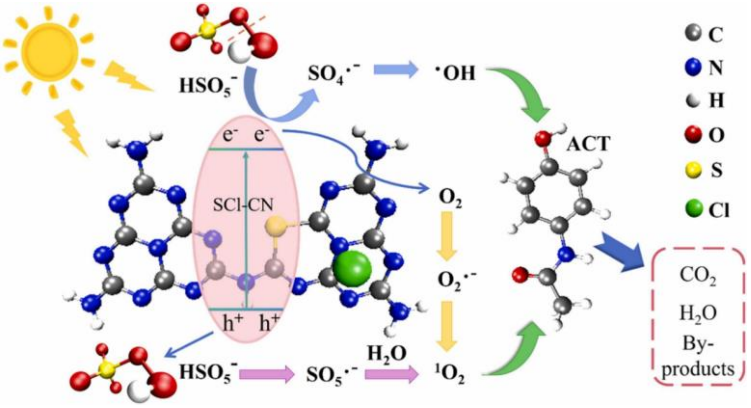

Figure 3: PMS activation under photocatalysis in the SCl-CN/PMS/ visible light system [43].

3.1.3. Electrochemical Activation

Electrochemical enhancement strategies have been proven to significantly improve PMS activation efficiency by promoting interfacial electron transfer and metal redox cycles, providing a new approach for pollutant degradation [44]. Electrochemical reactions primarily occur at the electrode interface. In anodic reactions, electrons are typically directly transferred to the PMS, where oxidation reactions occur to generate $SO_4^{\cdot-}$ and degrade pollutants. A study employed the drop-casting method to prepare a novel $CuBi_2O_4$ anode. The $CuBi_2O_4$ anode/PMS system achieved a degradation efficiency of 74.60% for the herbicide prometryn. The mechanism of electro-activation of PMS by $CuBi_2O_4$ anode is shown in Fig. (**4**) [45]. Additionally, due to the activation of water molecules on the anode surface, the system often generates ·OH, which further react with PMS to form $SO_4^{\cdot-}$ [46]. In the cathodic reaction, transition metals and electron-rich carbon-based cathodes can transfer electrons to PMS, breaking the O-O bond and forming $SO_4^{\cdot-}$ [47]. A study fixed 1T/2H-MoS_2 on carbon paper (carbon fiber cloth) as the cathode, forming a 1T/2H-MoS_2@CFC cathode/PMS system, achieving removal efficiencies of 55.1% and 54.0% for carbamazepine and phenol, respectively, within 90 minutes [48]. A $MoSe_2$/CNC cathode prepared by the hydrothermal method was used to construct an EC/$MoSe_2$@CNC cathode/PMS system, which achieved removal rates of 99.11%, 100%, and 91.54% for norfloxacin, Cu, and TOC within 60 minutes [44].

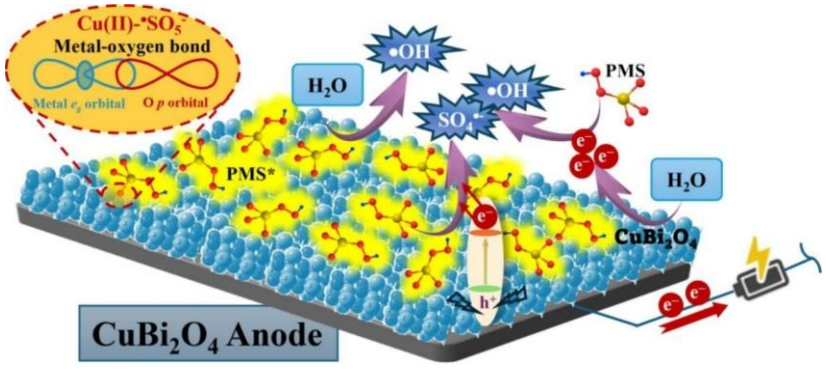

Figure 4: Schematic diagram of the mechanism of electro-activation of PMS by $CuBi_2O_4$ anode [45].

Current density is also an important parameter for electro-activated PMS. Current density exhibits a significant positive correlation with PMS activation efficiency, and increasing current density can accelerate radical generation [49]. For example, when the current density was increased from 8 mA/cm^2 to 32 mA/cm^2, the degradation rate

constant of acidic dye wastewater increased by 2.95 times [50]. However, beyond a critical value, efficiency growth slows down, and even decreases due to side reactions such as hydrogen evolution [51], thereby limiting practical application benefits. For example, in a study on the electro activation of PMS for the degradation of sulfamethoxazole (SMX), when the current density was increased from the optimal value of 5 mA/cm^2 to 10 mA/cm^2, the degradation rate constant of SMX decreased from 0.0870 to 0.0531, a reduction of 39% [52]. Different experimental systems require the selection of appropriate current densities based on specific requirements. Additionally, NaCl as an electrolyte typically exhibits better degradation performance [44]. This may be attributed to Cl^- generating active chlorine ($HClO/ClO^-$) at the anodized surface, which reacts with PMS to produce active free radicals, as detailed in Section 4.4.

It is worth mentioning that waste lithium-ion batteries (LIBs) are rich in leachable transition metals (such as Co, Ni, Mn), and recycling them to prepare PMS activation catalysts has become a green approach to achieving synergistic effects between resource regeneration and AOPs [53-55].A study utilized $LiCoO_2$ electrode waste from LIBs to activate PMS, simultaneously achieving the rapid degradation of 2,4,6-trichlorophenol (TCP) and the removal of ammonia nitrogen (NH_4^+-N) [14].

3.1.4. Plasma Activation

Low-Temperature Plasma (LTP) technology, primarily generated through methods such as gliding arc discharge, dielectric barrier discharge (DBD), corona discharge, and glow discharge, represents an emerging approach for activating PMS [56]. Characterized by its non-thermal equilibrium properties (where electron temperature significantly exceeds gas temperature), mild reaction conditions, high reactivity, and rapid initiation, this technology provides a novel pathway for the efficient activation of PMS to degrade organic pollutants [57]. The core mechanism of LTP-activated PMS for organic wastewater treatment lies in utilizing the combined effects generated during plasma discharge [58]. These effects include high-energy electrons, excited species, UV radiation, and localized high-temperature microzones, which collectively facilitate the efficient activation of PMS molecules [59]. This process primarily generates highly oxidizing $SO_4^{\cdot -}$ and ·OH [60]. Concurrently, the accompanying UV photolytic action and localized thermal effects synergistically contribute to the degradation of organic pollutants [61].

However, despite its high reactivity, plasma technology often exhibits the limitation of poor reaction selectivity when applied alone [57]. To overcome this drawback and further enhance degradation efficiency, coupling LTP with PMS, or further introducing catalysts (e.g., carbon-based materials) to construct a synergistic catalytic system, has emerged as an effective strategy. Typical studies of PMS activation by LTP are summarized in Table **2**. Notably, coupling LTP with carbon nanotubes (CNTs) not only significantly alters the electronic characteristics (e.g., work function, electron density) and surface functional groups of the material, but also enables the directed modulation of the oxidation mechanism within the PMS activation system [62, 63]. As illustrated in Fig. (**5**), when CNTs subjected to O_2 plasma etching are employed as catalysts, the contribution of the non-radical oxidation pathway dominated by singlet oxygen ($^1O_2$) to pollutant degradation increases substantially from 9.8% to 54.9% [64]. This shift effectively transitions the oxidation pathway from radical-dominated to non-radical-dominated.

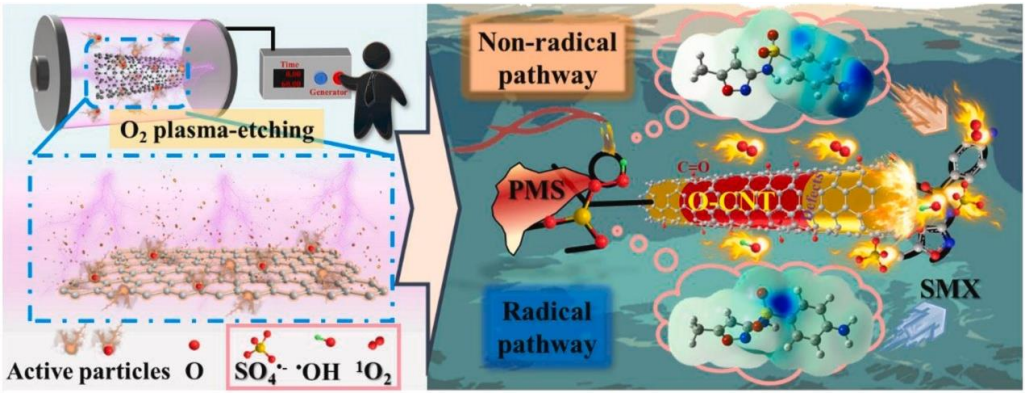

Figure 5: Schematic diagram of O_2 plasma-etched CNTs and their activation of PMS for oriented singlet oxygen production [64].

Table 2: Typical studies of PMS activation by LTP technology.

Activation Technologies	Treatment Objects	Treatment Effects	Dominant ROS	Ref.
Ar plasma-etching carbon nanotube	Sulfamethoxazole	The TOC removal was 42.5%, which is 4.6 times higher than the reaction rate constant of the conventional CNT/PMS system.	$^1O_2$	[58]
DBD plasma	Chlortetracycline	The removal rate of the coupled DBD/PMS system was 81.9%, which was 23.2% higher than that of the conventional PMS system, and the energy yield was 13.1% higher.	·OH	[60]
DBD plasma	Gatifloxacin	The removal of gatifloxacin by DBD/PMS system was about 96.3%. The synergistic coefficient was about 1.39, indicating a significant synergistic effect of DBD plasma on the activation of PMS.	·OH and $SO_4^{\cdot-}$	[65]
DBD plasma	Levofloxacin	At pH 8.7, levofloxacin degradation reached 94.1% and TOC removal 43.8%, which were 2.52 and 2.79 times higher than that of conventional aeration, respectively.	·OH and $^1O_2$	[66]
DBD plasma	Perfluorooctanoic acid	The degradation and defluorination rates of the DBD-PMS system reached 99.2% and 96.96%, respectively, which were significantly higher than those of the DBD plasma treatment alone (90.33%, 61%).	·OH	[67]
DBD plasma	Potassium ethyl xanthate	The degradation efficiency of potassium ethyl xanthate in the combined DBD/PMS system for 25 min was about 90.5%, which was significantly higher than that of the DBD and PMS systems alone (70.5% and 9.5%), showing a significant synergistic effect.	·OH and $SO_4^{\cdot-}$	[68]
Liquid-phase plasma	Sulfamethoxazole	The degradation efficiency of PMS/liquid-phase plasma is 1.35 times higher than that of liquid-phase plasma alone, and the TOC removal rate is approximately 2.5 times higher.	·OH	[69]
N_2 plasma-etching CNTs	Phenol	The degradation rate constant for phenol in the N-CNT-60/PMS system (0.1269 min^{-1}) was 10 times higher than that of the original MWCNT/PMS system.	$^1O_2$	[62]
O_2 plasma-etching CNTs	2,4-dichlorophenol	Degradation of 2,4-dichlorophenol reached 97% in 20 min, with a degradation rate 4.1 times higher than that of the conventional carbon nanotube.	$^1O_2$	[64]
O_2 plasma-modified CNTs	Sulfamethoxazole	The O-CNT-60/PMS system completely degraded sulfamethoxazole in 40 min with kobs of 0.09557 min^{-1}, which is 5.5 times higher than the original MW/CNT.	$^1O_2$ and $SO_4^{\cdot-}$	[63]
Plasma Electrolytic Oxidation treated 2-D black TiO_2	Tetracycline	The tetracycline degradation rate constant of the synergistic system reached 17.33 × 10^{-3} min^{-1} with a synergy factor of 2.10, which was significantly better than d single system (1.40).	·OH and $SO_4^{\cdot-}$	[61]
Underwater bubbling plasma and diatomite-$CoFe_2O_4$	Ciprofloxacin	Degradation of ciprofloxacin was 94.7% in 30 min with a kinetic constant of 0.097 min^{-1} and an energy efficiency of 145.2 mg/kW · h.	·OH	[70]
Water surface plasma (WSP)	Ciprofloxacin	The ciprofloxacin removal efficiency of the WSP/PMS system increased from 50.9% to 96.6% with a synergy factor of 3.224 and a kinetic constant of 0.113 min^{-1} for WSP alone.	·OH	[71]

3.2. Metal-based Materials Activation

3.2.1. Homogeneous System Activation

Transition metal ions (e.g., Co^{2+}, Fe^{2+}, Pd^{2+}, Cu^{3+}, Ni^{3+}) are widely used to activate PMS systems due to their high catalytic activity and operational convenience [72-76]. The Pd^{2+}/PMS system can achieve a degradation efficiency of 100% for phenolic compounds (4-Chlorophenol, dichlorophenol, and trichlorophenol) within 5 minutes [74]. The electron transfer cycle between metal ions is a key factor in activating PMS to generate ROS for the removal of organic pollutants; however, this cycle is often hindered to varying degrees in actual experimental environments [77]. Researchers typically use reducing agents (such as boron, hydroxylamine, and cysteine) or chelating agents

(such as citric acid, protocatechuic acid, and sinapic acid) to enhance the recycling efficiency of metal ions [17, 78-82]. As shown in Fig. (**6**), the addition of citric acid promotes the cycle of Fe(II) and Fe(III) in a homogeneous PMS system, which is more efficient in activating PMS and thus produces more ROS [80]. This type of homogeneous activation process does not require complex equipment and has potential for large-scale application. However, the leaching of metal ions poses a risk of secondary pollution, limiting its practical environmental application [83]. Therefore, researchers often employ strategies such as using metal oxides, constructing metal-organic framework (MOF), and adding suitable carriers to enhance `the system's catalytic activation performance for PMS.

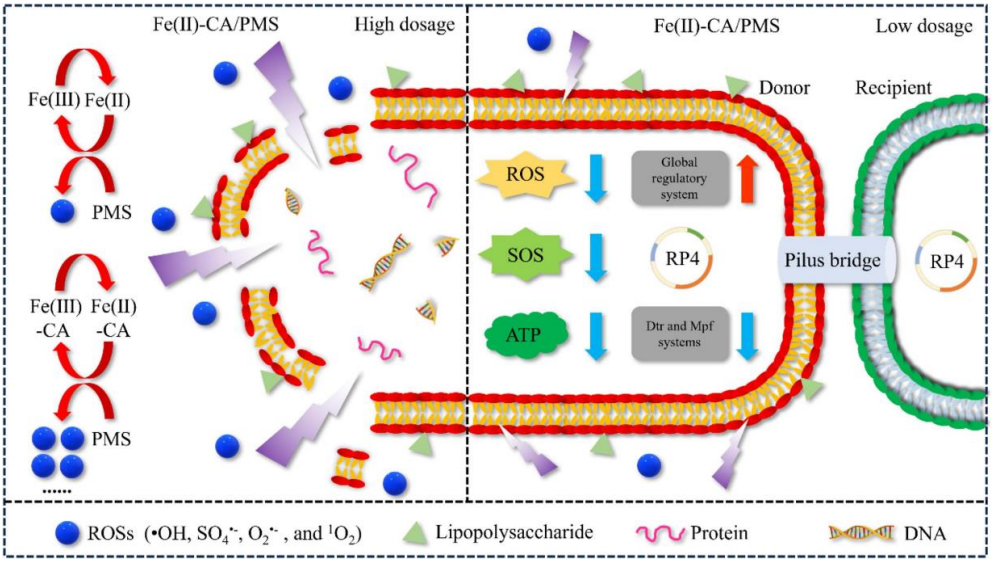

Figure 6: Schematic diagram showing that citric acid enhances the Fe(II) and Fe(III) cycle and that the Fe(II)-CA/PMS system inhibits antibiotic-resistant bacteria (ARB) and antibiotic resistance genes (ARG) [80].

3.2.2. Heterogeneous System Activation

In the field of PMS heterogeneous activation, metal oxides have attracted considerable attention as commonly used catalysts. Similar to homogeneous systems, the catalytic activity of metal oxides mainly depends on the redox cycle of metal ions $Me_{(n)}^{+}/Me_{(n+1)}^{+}$ [84]. At the same time, the electronic structure characteristics and defect state of the catalyst itself have a significant regulatory effect on the decomposition efficiency of PMS and the generation of ROS [18]. Compared to single-metal oxide systems, bimetallic oxides exhibit superior performance advantages in PMS activation. This is attributed to the dynamic electron transfer mechanism between the two metals. This mechanism not only enables synergistic catalytic effects between the two metals and promoting efficient redox reactions, but also maintains the stability of the catalytic cycle through continuous electron transfer, as shown in Fig. (**7**) [8]. In the degradation study of bisphenol A, the treatment effect of the Cu-Mn bimetallic $CuMnO_2$/PMS system was 5 times and 21 times higher than the Mn_2O_3/PMS and Cu_2O/PMS single metal systems [85].

Traditional bimetallic oxides often face challenges of insufficient structural stability due to their low lattice energy [86]. By inducing phase transformations through high-temperature calcination (>600°C), these systems can be restructured into stable structures such as perovskite (ABO_3) or spinel (AB_2O_4). The ordered occupation of B-site cations and strong metal-oxygen bond energies significantly suppress metal leaching, thereby enhancing the catalytic cycle stability [87, 88]. MOF composites and their derivatives, with their multi-level pore structures and dispersed metal sites, can significantly improve mass transfer efficiency while effectively suppressing the agglomeration of active components and metal leaching in traditional metal/metal oxide catalysts [89, 90]. Additionally, heteroatom doping is expected to enhance the performance of PMS in degrading organic pollutants by altering electronic structures and reconfiguring catalytic sites. Sulfur doping promotes the conversion of low-spin Co to high-spin Co. It increases the internal electron escape probability of Co_3O_4, which enhances the activation effect of PMS, achieving a removal rate of 96.4% for ofloxacin within 20 minutes [91]. Table **3** shows the studies on the activation of PMS by related metal-based catalysts.

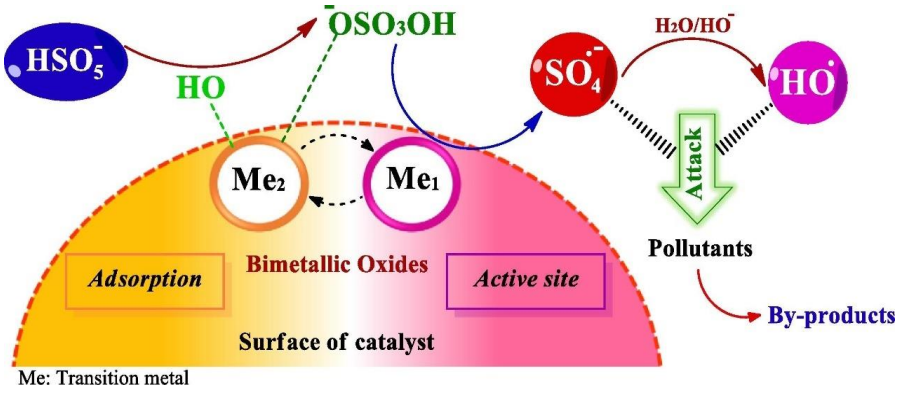

Figure 7: Transition metals activation of PMS on the surface of catalyst [8].

Table 3: Typical studies of PMS activation by metal-based catalysts.

Activation Technologies	Treatment Objects	Treatment Times	Treatment Effect	Ref.
$Bi_2Fe_4O_9$	Metronidazole	10 min	100% degradation of MTZ (5 mg/L). The reaction rate constant of 0.7629 1/min was significantly better than that of the single PMS system (0.025 1/min)	[92]
CoCuAl-LDH	Rhodamine B	15 min	>98% degradation of Rh B (100 mg/L). Copper can improve the conductive efficiency of CoAl-LDH.	[93]
CoFe-LDH	Acid Red 27	15 min	95% degradation. The degradation efficiency of CoFe-LDH was nearly twice that of conventional flake LDH (F-LDH).	[94]
Co_3O_4@LDH-AC	Levofloxacin	4 min	100% degradation. Degradation efficiency for actual hospital wastewater (COD> 150 mg/L) is maintained at more than 90%.	[95]
$FeCo_2O_4$	Ethylparaben	30 min	94.6% degradation and 40.5% TOC removal efficiencies were achieved.	[6]
Fe-Mn DAC	2-chlorophenol	5 min	100% degradation of 2-CP. Nearly 100% selectivity of high-valent metal oxides with 100% PMS utilization efficiency.	[96]
Fe-5Cu	4-chlorophenol	120 min	92% degradation, 62% dichlorination and 60% mineralization.	[15]
MOF/ CoS_2@C-3	Ciprofloxacin	10 min	>90% degradation of CIP (10 mg/L). The system demonstrated exceptional resistance to humic acid (HA), significant environmental stability, and a wide range of pH adaptation.	[97]
MOF/CuFe-N	Rhodamine B	30 min	99.5 % degradation of Rh B, with a mineralization rate of 60 %.	[98]
MOF/Cu-Fe	Tetracycline, phenol, etc.	30 min	>95% degradation. Among them, phenol was degraded by 100% in a wide pH range of 5~9, and the mineralization efficiency reached 70%.	[99]
MOF/Fe-Co	Sulfamethoxazole	30 min	100% degradation of SMX (5 mg/L). $SO_4\cdot^-$ and $^1O_2$ played a critical role in the degradation of SMX.	[100]
MOF/PDA-CoNi	Tetracycline hydrochloride	30 min	99.2% degradation of THC (15 mg/L). TOC removal rate of 61.8%.	[101]
$NiCo_2O_4$	Diclofenac	10 min	99.9% degradation and 97.2% mineralization were achieved.	[16]
ZIF-67/Co_xB@NC-450	Tetracycline	30 min	Achieving a degradation efficiency of 96% and a rate constant of 0.210 min^{-1}. The removal rate of TC from actual water bodies exceeds 85%.	[102]
ZIF-67/Co_3O_4@ CNT	Phenolic compounds	15 min	The mineralization of high EDC pollutants (hydroquinone, p-methoxyphenol) by the system was 83.63%, which was significantly better than single Co_3O_4 or CNT.	[103]
ZIF-67/Co-Fe@PBA	Metronidazole	15 min	>98% degradation of MNZ, Both MNZ and its intermediates exhibit significantly reduced levels of acute toxicity, developmental toxicity, and mutagenicity; notable secondary contamination.	[104]
ZIF-67/PBA@SiO_2	Levofloxacin	30 min	95.5% degradation of LEV (20 mg/L). The system exhibits strong anti-interference ability and ecological environment safety.	[105]

3.3. Carbon-based Material Activation

As a metal-free catalytic strategy, carbon-based materials (graphene, CNTs, activated carbon, and biochar, etc.) leverage their excellent adsorption properties and electronic conductivity to efficiently activate PMS, realizing effective degradation of organic pollutants [106]. The core mechanism of activation lies in the oxygen-containing functional groups (e.g., carboxyl and carbonyl groups) on the material surface adsorbing PMS (HSO_5^-) through hydrogen bonding or electrostatic interactions. This forms peroxide-like intermediates (C=O···HSO_5^-, PMS*), which then trigger a pollutant oxidation degradation pathway dominated by non-radical ($^1O_2$) species [107]. These materials are widely available and cost-effective, offering a promising environmentally friendly technological approach for environmental pollution control. Biomass carbon microcoil aerogels (BCCA) activated PMS exhibit the advantages of low cost, ultra-lightweight, high elasticity, and recyclability. Within 10 minutes, the removal efficiency for methylene blue and methyl orange exceeded 95%, and within 90 minutes, the removal efficiency for tetracycline reached 96.5% [108]. Activated carbon fiber (ACF) activated PMS treated coking wastewater, achieving removal rates of 76%, 98%, and 98% for COD, pH, and color, respectively. At the same time, the biochemical oxygen demand to chemical oxygen demand ratio (BOD_5/COD) of the wastewater significantly improved from 0.16 at the initial stage to 0.72, and its biodegradability was greatly improved [109].

Composite catalytic systems constructed with carbon-based materials and metal-based materials can effectively solve problems such as metal ion leaching and recovery difficulties in traditional metal catalysts [110-112]. By introducing carbon-based carriers, composite materials can be designed with unique structures such as core-shell structures and limited loading to prevent active particle agglomeration [88, 113]. The system primarily relies on the excellent electron transfer ability of metal ions and the strong oxidizing properties of $^1O_2$ to degrade pollutants, as shown in Fig. (**8**). A study prepared a $Fe(acac)_3$@ZIFs catalyst with a dodecahedral structure dispersed in a porous carbon framework using iron acetylacetonate-coated zeolite imidazole as the raw material. This catalyst exhibits excellent stability with minimal iron ion leaching. It achieved an effective degradation of 87.20% of pharmaceutical pollutants in actual hospital wastewater [114].

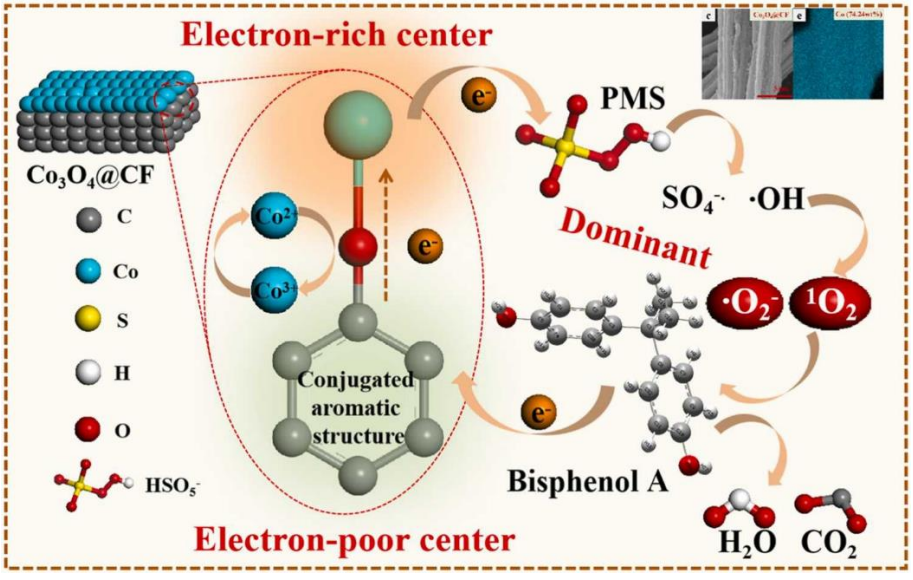

Figure 8: Schematic diagram of Co_3O_4@CF-activated PMS degradation of phenolic pollutants [115].

Additionally, structural defects (e.g., edge sites, vacancies) and doped heteroatoms (N, S, P) in the carbon framework can alter the electronic distribution of the material, forming electron-rich centers and enhancing the catalytic activity for PMS [116-118]. A study demonstrated that nitrogen-doped graphene-loaded ruthenium (N-rGO-Ru) catalyst achieved a removal efficiency of 92% for sulfamethoxazole within 120 minutes, significantly higher than that of N-rGO/PMS (74%) and rGO/PMS (70.11%) [119]. Doping nitrogen into cobalt phosphide-based materials to activate PMS achieved a removal efficiency of up to 92.3% for tetracycline (TC) within 30 minutes, which is 1.85 times higher than CoP@C/NF/PMS system [120].

3.4. Composite System Activation

Through the synergistic effect of electrochemistry and metal-based catalysts, PMS-AOPs can be efficiently activated to achieve significant degradation of organic pollutants [121]. Manganese oxide-carbon modified graphite felt (MnO-C/GF) was used as an anode to activate PMS under electrochemical synergism. The degradation rate constants (*k*) of tetracycline were increased by a factor of 4.54 and 2.38 compared to GF and MnO/GF, respectively [121].

The system combining metal-based catalysts with photocatalytic Fenton reactions exhibits excellent PMS activation performance [122, 123]. A study used Mn/Fe bimetal-doped graphitic carbon nitride (MnFe-CN-50) as a catalyst in a visible light/PMS synergistic system, the degradation efficiencies of tetracycline were 2.6 times and 1.3 times higher than those in standalone photocatalysis or Fenton-like reactions [124].

The triple synergistic effect of photocatalysis, electrochemistry, and metal-based catalysts not only significantly improves the degradation efficiency of pollutants by enhancing ROS generation, but also promotes energy recovery [125]. A study achieved simultaneous activation of PMS and H_2O_2 using sulfur-doped CuMnO/carbon felt cathodes (Fig. **9**), and the removal rate of rifampicin and TOC were 96.9% and 78.1%, respectively, within 15 minutes [126]. This synergistic effect enables the dual functions of "wastewater purification + power generation", showing great promise for energy-self-sufficient wastewater treatment and energy recovery.

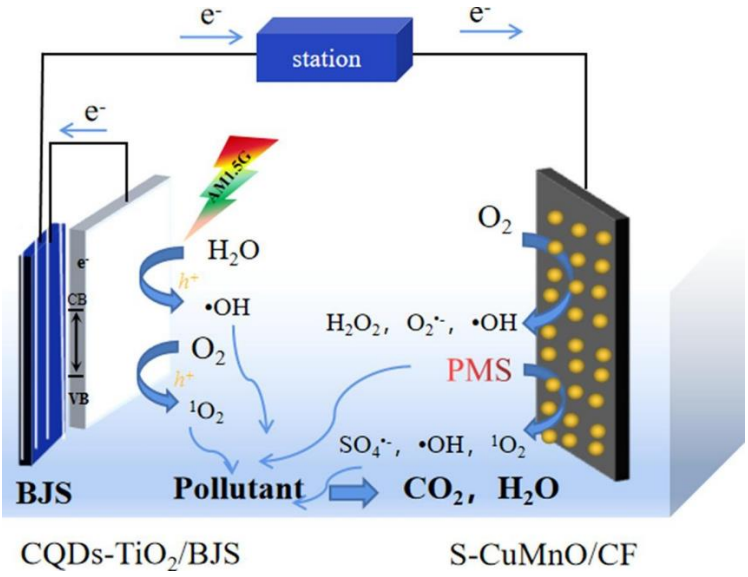

Figure 9: Simultaneous activation of PMS and H_2O_2 by S-CuMnO/CF [126].

While PMS-AOPs exhibit high degradation efficiency, their economic viability depends on catalyst recyclability and energy input optimization. Future studies should focus on low-cost catalysts (e.g., waste-derived materials) and hybrid systems (e.g., solar-driven activation) to enhance sustainability [127-130].

4. Critical Parameters that Affect PMS-AOPs Performance

4.1. Initial pH of Wastewater

The pH of wastewater significantly influences PMS performance by regulating the generation pathways of reactive species, the surface charge of catalysts, and the speciation of pollutants [131]. Under acidic conditions, metal ions exhibit higher activation efficiency toward PMS in homogeneous systems, as low pH promotes metal dissolution and cycling (such as Fe^{3+}/Fe^{2+}) [132]. Here, $SO_4^{\bullet-}$ serves as the dominant reactive species, demonstrating strong reactivity toward organic compounds. In neutral to weakly alkaline conditions, $SO_4^{\bullet-}$ can hydrolyze to form ·OH, establishing a dual-radical synergistic system that broadens the degradation scope of pollutants [17]. Under strongly alkaline conditions, non-radical pathways (dominated either by direct nucleophilic

attack or $^1O_2$) may prevail, whereas accelerated spontaneous decomposition of PMS leads to inefficient consumption [133]. Furthermore, pH variations affect the zeta potential of carbon-based catalysts, thereby altering their adsorption behavior toward PMS and pollutants [134]. Therefore, pH optimization is essential based on the activation mechanism and target pollutant characteristics.

4.2. Reaction Temperature

High temperatures can enhance PMS activation rates by accelerating molecular motion. It is widely observed that pollutant degradation rates increase linearly following the Arrhenius equation within 20 – 80°C [19]. Breakthrough research reveals a unique freezing concentration effect in cryogenic zones (-40 – 0°C), where direct PMS oxidation dominates pollutant degradation [135, 136]. For eight representative pollutants including Acid Yellow 17, removal efficiencies exhibit a rising-falling pattern as temperature increases from -40°C to 0°C, peaking at -20°C. Overall, across the full temperature spectrum (-40 – 80°C), degradation curves display an N-shaped trend (Fig. **10**), with all three stages conforming to pseudo-first-order kinetics [137]. This demonstrates temperature's nonlinear modulation of reaction pathways and provides new strategies for wastewater treatment in cold regions.

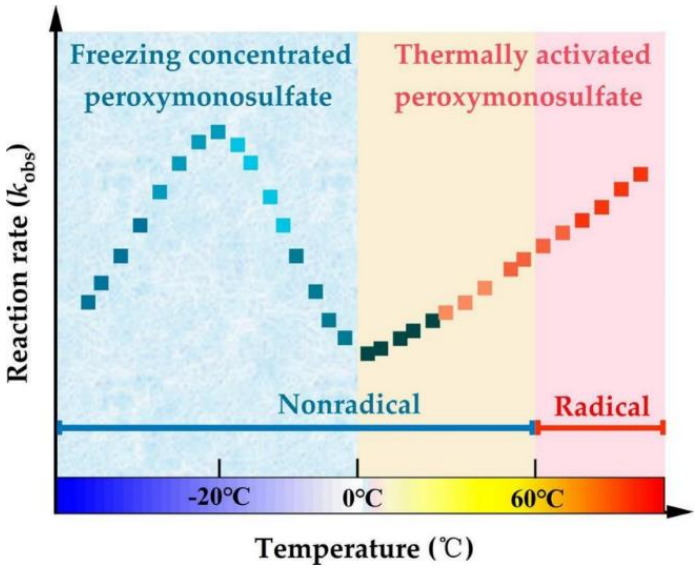

Figure 10: Trend of organic pollutants within -40 – 80°C in PMS-AOPs system [137].

4.3. PMS Dosage and Catalyst Loading

The PMS dosage is a critical parameter determining both the upper limit of reactive species generation and process economics. At low dosages, the pollutant degradation rate typically increases linearly with PMS concentration, conforming to the pseudo-first-order kinetic model [138]. When PMS is in excess, degradation efficiency may plateau or even decline due to triggered self-quenching reactions of PMS (Eqs. (4), (5)) and/or competitive consumption of SO4·-/·OH by excessive PMS that competes with target pollutants (Eqs. (6), (7)) [139]. Additionally, accumulation of reaction byproducts can suppress radical chain reactions.

$$SO_4^{\cdot-} + SO_4^{\cdot-} \rightarrow S_2O_8^{2-\cdot} \quad (4)$$

$$SO_4^{\cdot-} + S_2O_8^{2-} \rightarrow SO_4^{2-} + S_2O_8^{2-\cdot} \quad (5)$$

$$SO_4^{\cdot-} + HSO_5^- \rightarrow SO_5^{\cdot-} + HSO_4^- \quad (6)$$

$$SO_4^{\cdot-} + HSO_5^- \rightarrow SO_5^{\cdot-} + HSO_4^- \quad (7)$$

The catalyst loading directly influences the number of active sites and mass transfer efficiency. At low loadings, the degradation rate increases with catalyst amount through enhanced PMS activation by additional active sites

[140]. However, excessive loading often reduces efficiency through induced particle agglomeration diminishing effective surface area, amplified light shielding in photocatalytic systems, or surplus catalyst acting as electron sinks that impede pollutant oxidation in non-radical pathways [141]. Furthermore, overdosing metal-based catalysts exacerbates ion leaching risks.

4.4. Inorganic Ions and Natural Organic Matter

With advances in activation technologies and materials, the stability of reaction systems has progressively improved. These systems now demonstrate significant tolerance and buffering capacity toward inorganic anions (PO_4^-, HPO_4^{2-}, HCO_3^-, NO_3^-, Cl^- at 1 – 10 mM) and humic acid (HA), exerting generally negligible effects on PMS activation as shown in Fig. (**11**) [114, 142].

The slight inhibition by $H_2PO_4^-$ may primarily stem from its reaction with radicals forming less reactive H_2PO_4· species (Eqs. (8), (9)) [143]. For HCO_3^-, observed inhibition arises through dual mechanisms: (i) consuming reactive species to generate lower-activity radicals (HCO_3·/CO_3^-·; Eqs. (10), (11)), (ii) pH buffering toward weak alkalinity that alters pollutant degradation pathways [144]. When HA exhibits inhibitory effects, potential causes include surface adsorption blocking catalyst active sites or competitive consumption of reactive species [114]. Conversely, HA may enhance degradation *via* reductive functional groups (e.g., phenolic hydroxyls) reacting with PMS to generate additional reactive species [145].

$$HPO_4^{2-} + SO_4^{\cdot-} \rightarrow SO_4^{2-} + HPO_4^{\cdot-} \quad (8)$$

$$HPO_4^{2-} + \cdot OH \rightarrow OH^- + HPO_4^{\cdot-} \quad (9)$$

$$HCO_3^- + SO_4^{\cdot-} \rightarrow SO_4^{2-} + HCO_3 \cdot \quad (10)$$

$$HCO_3^- + \cdot OH \rightarrow CO_3^{\cdot-} + H_2O \quad (11)$$

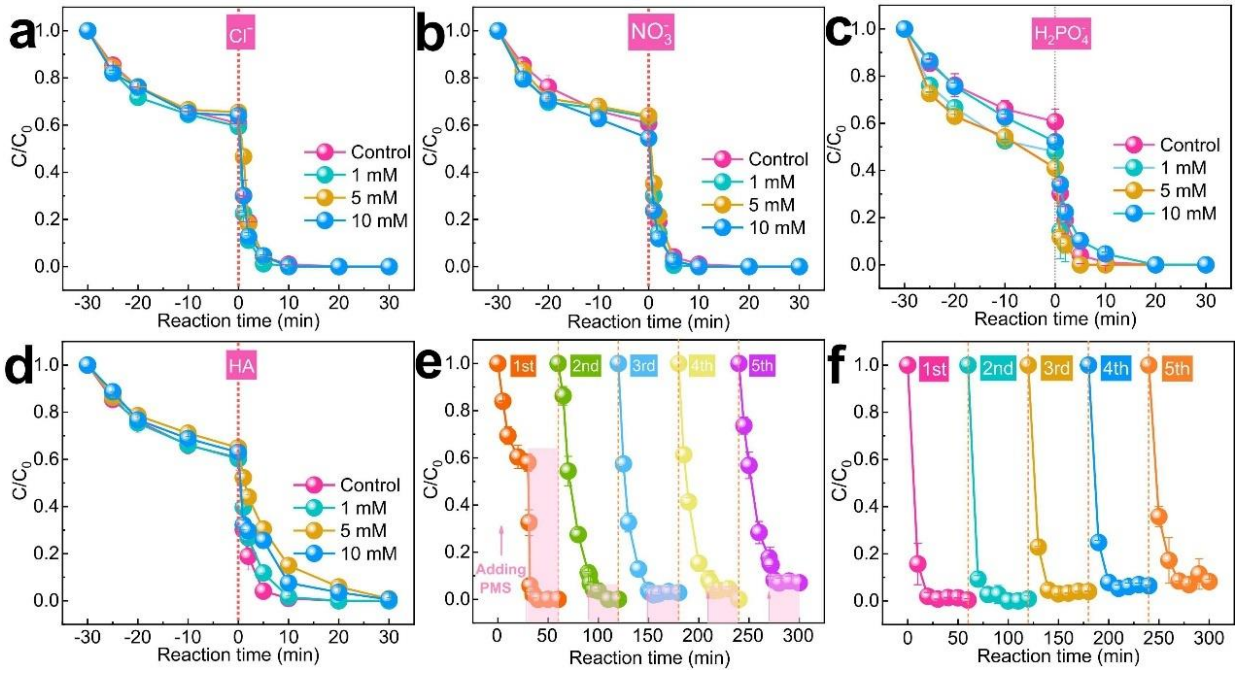

Figure 11: Effect of inorganic anions and HA on sulfafurazole removal (The negative x-axis indicates the adsorption stage) [114].

Low concentrations of Cl^- exhibit minimal impact on PMS-AOP degradation efficiency, but appropriate Cl^- concentrations can directly activate PMS to generate reactive species. In Cl^-/PMS systems without catalysts, the primary oxidizing agents are typically hypochlorous acid (HOCl) and reactive chlorine species (Cl·) formed through

direct oxidation between Cl^- and PMS [145, 146]. Notably, a study demonstrated 100.0% degradation efficiency for ammonium nitrogen (NH_4^+-N) and 97% removal of total nitrogen (TN) within 15 minutes in seawater aquaculture wastewater using a Cl^-/PMS system at pH 8.0 [147]. Moreover, introducing Cl^- significantly enhances the activation performance of catalyst/PMS systems. Research reveals that in PMS systems, Cl^- promotes the generation of Fe (IV)=O species on single-atom Fe-CNs catalysts, increasing sulfamethoxazole degradation by 2.97-fold and boosting PMS utilization efficiency by 92%. At the same time, this approach effectively prevents the formation of chlorinated organic by-products [148].

In PMS systems containing multiple halogens, the presence of X_1^- promotes the transformation of HOX_1/OX_1^- into HOX_2/OX_2^- species with higher oxidizing capacity. Environmental temperature significantly modulates the conversion of X^- to HOX/OX^- in X^-/PMS systems. Research demonstrates that Cl^- substantially enhances degradation efficiency across tested temperature ranges [137], whereas Br^- addition mediates the transformation of primary active species from HOCl/OCl^- to HOBr/OBr^-. This shift amplifies the oxidizing capacity of X^-/PMS systems, with performance exhibiting positive correlation to temperature elevation [149].

Therefore, we boldly speculate that when treating halogenated organic wastewater, PMS may be able to produce activity without additional activation conditions in a non-catalytic system. And it tends to degrade organic compounds with electron-donating properties, low molecular polarity, and low oxygen content [150]. This can effectively solve problems such as resource waste and high treatment costs.

4.5. Reaction Time

Reaction time is a critical parameter determining the extent of target pollutant degradation and the operational efficiency of the system. In PMS-AOPs, pollutant degradation typically follows pseudo-first-order or pseudo-second-order kinetic models [151, 152]. Degradation efficiency often increases rapidly with time during the initial reaction stage, peaks, and then stabilizes or slightly declines [24, 28]. In the initial phase, sufficient reactive species (such as $^1O_2$, $SO_4^{\cdot-}$, and ·OH) and available active sites on the catalyst ensure a significant increase in pollutant degradation rate over time [94, 101].

The reaction time required varies significantly depending on the activation method, influenced by the activation efficiency, the rate of reactive species generation, and the inherent degradability of the pollutant itself. Energy-assisted activation (e.g., thermal, photocatalytic, electrochemical and plasma) and efficient heterogeneous metal/carbon-based catalysts can typically achieve high degradation efficiency (>90%) within a relatively short timeframe (<30 minutes, often even <10 minutes) [24, 34, 50, 120, 124]. In contrast, some homogeneous systems or reactions under specific conditions may require longer durations (e.g., >120 minutes) to achieve satisfactory removal [15]. Determining the minimum effective time required for a specific system to reach the target removal efficiency is crucial for optimizing process economics.

Excessively long reaction times not only increase energy consumption and operational costs but may also lead to negative effects, primarily due to reactive species quenching, catalyst deactivation, and accumulation of by-products [139-141]. In practical applications, kinetic studies are necessary to determine the optimal reaction time required to achieve the expected removal rate. Selecting activation methods capable of achieving efficient degradation within a shorter timeframe is preferable [153]. A balance must be struck between degradation efficiency, energy consumption, treatment costs, and the potential risk of secondary pollution.

5. Working Mechanism of PMS

PMS activation primarily proceeds *via* three pathways for oxidative degradation of organic pollutants: radical-driven (·OH, $SO_4^{\cdot-}$, and $O_2^{\cdot-}$), non-radical-mediated ($^1O_2$, electron transfer, or high-valent metal species), and synergistic effects. The contributions of the three pathways depend on reaction conditions (temperature, pH, PMS concentration), catalyst composition and structure, pollutant properties, and analytical approaches [154]. Researchers typically employ radical quenching experiments, electron paramagnetic resonance, X-ray photoelectron spectroscopy, electrochemical analysis, and density functional theory (DFT) calculations to identify specific mechanisms [74].

The radical pathway primarily cleaves the O-O bond of PMS *via* electron transfer, generating $SO_4^{\cdot-}$ and ·OH. Concurrently, self-decomposition of PMS produces $O_2^{\cdot-}$ and $^1O_2$, which collectively degrade pollutants [155]. For biochar-activated PMS systems, radical pathways dominate with $SO_4^{\cdot-}$ and ·OH contributing approximately 70% to antibiotic degradation, $O_2^{\cdot-}$ exhibiting minimal contribution, while non-radical processes account for 15 – 20% [156]. Non-radical pathways (e.g., interfacial direct electron transfer) circumvent radical diffusion losses, demonstrating superior efficacy in complex water matrices [133]. In Zhou's study, it was found that steady-state concentration of $^1O_2$ is 4 orders of magnitude higher than radical ·OH [157]. It suggests that the dominant contribution of $^1O_2$ to BPA removal. Advancing research reveals that in PMS systems with metal ions, oxidative degradation is primarily mediated by metal-peroxo complexes rather than conventional species (·OH, $SO_4^{\cdot-}$, high-valent metals, or $^1O_2$) [72, 158]. The mechanism of action is as follows: first, PMS adsorbs onto the catalyst surface to form a metastable intermediate (PMS*); second, internal electron transfer occurs from the catalyst to the PMS molecule; finally, external electron transfer occurs from PMS* to pollutants [159]. In most cases, radical and non-radical pathways exhibit synergy in the PMS system, as shown in Fig. (**12**).

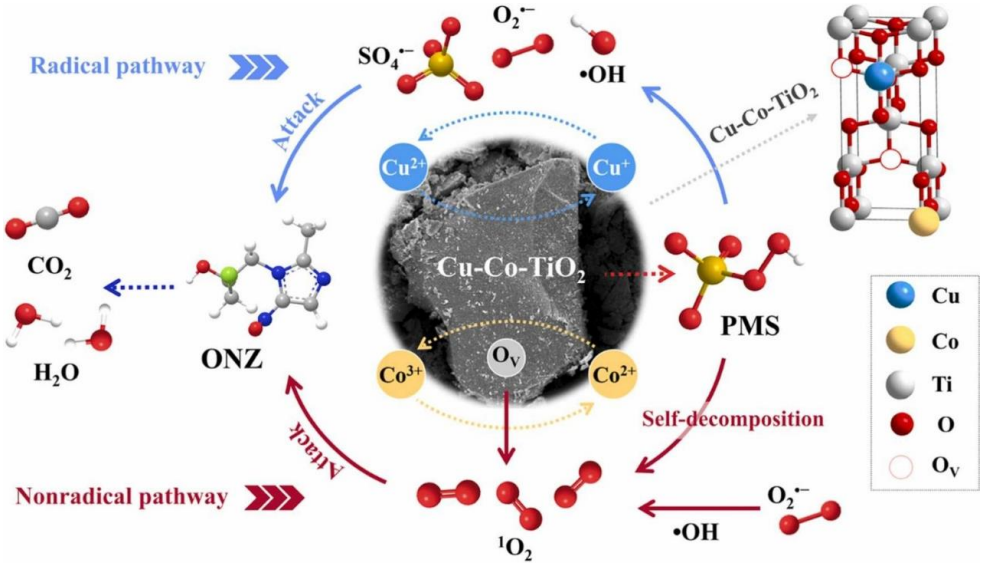

Figure 12: Mechanism of PMS activation on the surface of Cu-Co-TiO_2 catalyst [160].

6. Proposed Study Directions in the Near Future

(1) Develop carbon-based catalysts with defect engineering and single-atom doping synergistic regulation to improve catalytic stability and avoid the risk of metal ion leaching from metal-based materials.

(2) The structure, chemical behavior, and reaction mechanisms of critical oxidant PMS* in non-radical electron transfer pathways require further elucidation. Notably, pollutant degradation may originate not only from oxidants but also from high-energy catalyst states (e.g., high-valent metals), warranting investigation into catalytic active intermediates.

(3) Laboratory-scale validation of PMS catalyst tolerance toward inorganic anions and natural organics remains inadequate. Real-wastewater interference mechanisms demand clarification through in situ techniques (Raman/electron paramagnetic resonance) to decipher dynamic interactions between reactive species and matrices, enhancing complex-water adaptability.

(4) Although cryogenic “freezing concentration effects” intensify direct PMS oxidation, engineering application faces feasibility challenges. Development of freeze-resistant catalysts and optimized reactor mass-transfer designs is imperative.

(5) Waste-derived catalysts (e.g., spent lithium batteries, iron oxide ores) enable “waste-treats-waste” resource recovery. However, composition controllability and toxicity residuals necessitate standardized recycling-activation process chains.

(6) Deliberate regulation of radical/non-radical pathways requires deeper exploration. Transition from passive mechanistic analysis to proactive catalytic process design is crucial for advancing engineered PMS-AOPs applications.

7. Conclusions

The use of PMS in the treatment of refractory organic wastewater is comprehensively reviewed herein from some critical aspects, including the characteristics of PMS-AOPs, activation of PMS, effect parameters of PMS-AOPs, working mechanism of PMS, and study direction in the near future.

(1) PMS-AOPs show significant superiority in treating refractory organic wastewater relying on the production of reactive free radicals (SO_4·- and ·OH) and non-radical species ($^1O_2$), and wide pH operating range.

(2) PMS activation methods include energy-assisted activation (thermal, photocatalytic, electrochemical and plasma activation), metal-based materials activation (homogeneous/heterogeneous), carbon-based material activation, and synergistic activation of composite systems. The construction of a stable activation system with low secondary pollution risk (especially low cobalt/cobalt-free) and high water quality adaptability is important to achieving efficient treatment.

(3) The degradation efficiency is influenced by key parameters, including the initial pH of the wastewater, reaction temperature, PMS dosage, catalyst loading, coexisting inorganic ions and natural organic matter, and reaction time. These factors simultaneously influence the reaction process by regulating the surface properties of the catalyst and the generation of active species. Determining optimal reaction conditions is key to balancing the trade-offs among degradation efficiency, energy consumption, treatment cost, and secondary contamination risk.

(4) PMS activation primarily occurs through three pathways: radical-mediated, non-radical-mediated, and synergistic interactions between them. The non-radical pathway (particularly direct electron transfer mediated by 1O2 and PMS*) demonstrates superior interference resistance in complex aquatic environments.

(5) Future research should focus on the development of highly stable catalysts, the elucidation of the non-radical electron transfer mechanism, the enhancement of the adaptability to complex water qualities, and the exploration of the PMS-AOPs' application potential in low-temperature/halogenated wastewater scenarios.

Conflict of Interest

The authors declare that they have no known competing financial interests or personal relationships that could have appeared to influence the work reported in this paper.

Funding

This work was supported by the National Natural Science Foundation of China (grant number 51808039).

Acknowledgments

The authors also thank the anonymous reviewers for their helpful suggestions to improve the quality of our paper.

Data Availability

Data will be made available on request.

Author Contributions

Nannan Wang: Conceptualization, Funding acquisition, Project administration, Supervision, Writing – review & editing.

Ye Yang: Methodology, Validation, Writing – original draft

Kai Wang: Investigation, Visualization.

Xu Liu: Data curation, Formal analysis.

Zishan Hou: Validation.

Xiangyu Liu: Software.

Siquan Zou: Resources.

Zaixing Li: Supervision.

References

[1] Peng FJ, Feng XJ, Li S, Yu XL, Chen J, Liu SS*, et al.* Removal of emerging organic contaminants in a subsurface wastewater infiltration system: A preliminary study of microbial mechanism. Water Res. 2025; 284(11): 123960. https://doi.org/10.1016/j.watres.2025.123960

[2] Abonyi MN, Obi CC, Nwabanne JT. Degradation of organic pollutants in wastewater using MOF-based catalysts: A review. Next Materials. 2025; 8: 100696. https://doi.org/10.1016/j.nxmate.2025.100696

[3] Aasli B, El Messaoudi N, Miyah Y, Benjelloun M, Georgin J, Franco DSP*, et al.* A comprehensive review of the use of urea-formaldehyde resin composites for the adsorption of organic and inorganic pollutants from wastewater. Nano-Struct Nano-Objects. 2025; 43: 101495. https://doi.org/10.1016/j.nanoso.2025.101495

[4] Yin Z, Li Z, Deng Y, Xue M, Chen Y, Ou J*, et al.* Multifunctional CeO_2-coated pulp/cellulose nanofibers (CNFs) membrane for wastewater treatment: Effective oil/water separation, organic contaminants photodegradation, and anti-bioadhesion activity. Ind Crops Prod. 2023; 197: 116672. https://doi.org/10.1016/j.indcrop.2023.116672

[5] Xiangyu B, Chao L, Shilong H, jiping Z, Hu J. Combining advanced oxidation processes with biological processes in organic wastewater treatment: Recent developments, trends, and advances. Desalin Water Treat. 2025; 323: 101263. https://doi.org/10.1016/j.dwt.2025.101263

[6] Palas B. Catalytic performance of $FeCo_2O_4$ spinel cobaltite for degradation of ethylparaben in a peroxymonosulfate activation process: Response surface optimization, reaction kinetics and cost estimation. J Mol Struct. 2025; 1322: 140340. https://doi.org/10.1016/j.molstruc.2024.140340

[7] Zhao W, Shen Q, Nan T, Zhou M, Xia Y, Hu G*, et al.* Cobalt-based catalysts for heterogeneous peroxymonosulfate (PMS) activation in degradation of organic contaminants: Recent advances and perspectives. J Alloys Compd. 2023; 958: 170370. https://doi.org/10.1016/j.jallcom.2023.170370

[8] Kohantorabi M, Moussavi G, Giannakis S. A review of the innovations in metal- and carbon-based catalysts explored for heterogeneous peroxymonosulfate (PMS) activation, with focus on radical vs. non-radical degradation pathways of organic contaminants. Chem Eng J. 2021; 411: 127957. https://doi.org/10.1016/j.cej.2020.127957

[9] Peng Y, Tang H, Yao B, Gao X, Yang X, Zhou Y. Activation of peroxymonosulfate (PMS) by spinel ferrite and their composites in degradation of organic pollutants: A Review. Chem Eng J. 2021; 414: 128800. https://doi.org/10.1016/j.cej.2021.128800

[10] Tian H, Li C, Wang Z, Zhao S, Xu Y, Wang S. Polycyclic aromatic hydrocarbons degradation mechanisms in methods using activated persulfate: Radical and non-radical pathways. Chem Eng J. 2023; 473: 145319. https://doi.org/10.1016/j.cej.2023.145319

[11] Wang J, Wang S. Activation of persulfate (PS) and peroxymonosulfate (PMS) and application for the degradation of emerging contaminants. Chem Eng J. 2018; 334: 1502-1517. https://doi.org/10.1016/j.cej.2017.11.059

[12] Song H, Yan L, Wang Y, Jiang J, Ma J, Li C*, et al.* Electrochemically activated PMS and PDS: Radical oxidation versus nonradical oxidation. Chem Eng J. 2020; 391: 123560. https://doi.org/10.1016/j.cej.2019.123560

[13] Wacławek S, Lutze HV, Sharma VK, Xiao R, Dionysiou DD. Revisit the alkaline activation of peroxydisulfate and peroxymonosulfate. Curr Opin Chem Eng. 2022; 37: 100854. https://doi.org/10.1016/j.coche.2022.100854

[14] Feng L, Liao X, Wu M, Yuan Y, Ai Z, Zhang L*, et al.* Enhanced removal of ammonia induced by the co-existing halogenated organics in wastewater via reutilization of spent lithium-ion batteries for peroxymonosulfate activation. Chem Eng J. 2023; 470: 144430. https://doi.org/10.1016/j.cej.2023.144430

[15] Scaggiante G, Checa-Fernandez A, Zingaretti D, Dominguez C M, Santos A, Baciocchi R. Activation of peroxydisulfate and peroxymonosulfate by zero-valent iron and FeCu bimetals for 4-chlorophenol oxidation in water. J Water Process Eng. 2024; 68: 106446. https://doi.org/10.1016/j.jwpe.2024.106446

[16] Sampe K, Katsumata H, Tateishi I, Furukawa M, Kaneco S. Activation of peroxymonosulfate by morphologically modified $NiCo_2O_4$ and application to diclofenac degradation. Next Mater. 2025; 8: 100597. https://doi.org/10.1016/j.nxmate.2025.100597

[17] Wu Z, Zou J, Li S, He L, Li Q, Zhou Z*, et al.* Strong enhancement on tetrabromobisphenol A removal in natural water matrix by adding cysteine into Cu(II)/peroxymonosulfate system over the wide pH range of 4–12: Efficiency and mechanism. Chem Eng J. 2024; 501: 157548. https://doi.org/10.1016/j.cej.2024.157548

[18] Geng L, Geng F, Cheng X, Yang M, Wang X, Zhang Y Z*, et al.* Triggering efficient redox cycling and electron transporting in CuCo spinel oxides via oxygen vacancy building for rapid degradation of antibiotics. Chem Eng J. 2024; 500: 156731. http://dx.doi.org/10.1016/J.CEJ.2024.156731

[19] Dai Y, Wang B, Zhang M, Li W, Wang L, Zou Y*, et al.* Thermal activation of peroxymonosulfate for enhanced volatile fatty acids production and phosphorus release during anaerobic fermentation of iron-rich sludge. Bioresour Technol. 2025; 432: 132653. https://doi.org/10.1016/j.biortech.2025.132653

[20] Li N, Wu S, Dai H, Cheng Z, Peng W, Yan B*, et al.* Thermal activation of persulfates for organic wastewater purification: Heating modes, mechanism and influencing factors. Chem Eng J. 2022; 450: 137976. https://doi.org/10.1016/j.cej.2022.137976

[21] Ranaweera R, Wu X, Ng D, Reineck P, Zhang J, Williams M*, et al.* Comparative study of adsorption, thermally activated peroxymonosulfate and wet air oxidation for tetracycline removal and wastewater treatment. J Water Process Eng. 2025; 72: 107559. https://doi.org/10.1016/j.jwpe.2025.107559

[22] Wang L, Sun Z, Shi J, Li H, Fu T, Xu Y*, et al.* Selective oxidation of nitrogenous heterocyclic compounds by heat/peroxymonosulfate in phenol-rich wastewater. Water Res. 2025; 269: 122804. https://doi.org/10.1016/j.watres.2024.122804

[23] Liu P, Wu Z, Manzoli M, Cravotto G. Magnetic biochar generated from oil-mill wastewater by microwave-assisted hydrothermal treatment for sonocatalytic antibiotic degradation. J Environ Chem Eng. 2025; 13(1): 114996. https://doi.org/10.1016/j.jece.2024.114996

[24] Qu J, Liu R, Bi X, Li Z, Li K, Hu Q*, et al.* Remediation of atrazine contaminated soil by microwave activated persulfate system: Performance, mechanism and DFT calculation. J Cleaner Prod. 2023; 399: 136546. https://doi.org/10.1016/j.jclepro.2023.136546

[25] Sonawane S, Rayaroth M P, Landge V K, Fedorov K, Boczkaj G. Thermally activated persulfate-based Advanced Oxidation Processes — recent progress and challenges in mineralization of persistent organic chemicals: a review. Curr Opin Chem Eng. 2022; 37: 100839. https://doi.org/10.1016/j.coche.2022.100839

[26] Fan D, Hu M, Li S, Chen P, Jiang H, Tu X*, et al.* CNTs with nano-confined TiO_2 and surface loading Co_3O_4: The analysis of its performance and mechanism of PMS activation for ECs degradation under visible light. Sep Purif Technol. 2025; 352: 127840. https://doi.org/10.1016/j.seppur.2024.127840

[27] Wang H, Long Z, Chen R, Zhang H, Shi H, Chen Y. Boosting PMS activation over $BiVO_4$ piezo-photocatalyst to rapidly degrade tetracycline: Intermediates and mechanism. Sep Purif Technol. 2024; 331: 125598. https://doi.org/10.1016/j.seppur.2023.125598

[28] Hou C, Kang Y, Wang D, Xuan Y, Wang H, Li J*, et al.* Vis-light-driven activation of persulfate by $Bi_2Mo_xW_{1-x}O_6$: Elucidating the electronic mechanism for enhanced photocatalytic activity. J Alloys Compd. 2025; 1021: 179675. https://doi.org/10.1016/j.jallcom.2025.179675

[29] Chen H, Yin R, Zhu M. How to enhance persulfate processes by external-field effects: From fundamentals to applications. Water Res. 2025; 274: 123026. https://doi.org/10.1016/j.watres.2024.123026

[30] Alayande A B, Hong S. Ultraviolet light-activated peroxymonosulfate (UV/PMS) system for humic acid mineralization: Effects of ionic matrix and feasible application in seawater reverse osmosis desalination. Environ Pollut. 2022; 307: 119513. https://doi.org/10.1016/j.envpol.2022.119513

[31] Shen L, Wang H, Kang J, Shen J, Yan P, Gong Y*, et al.* Simultaneous elimination of N,N-dimethylhydrazine compounds and its oxidation by-product N-nitrosodimethylamine by UV-activated peroxymonosulfate process: Multiple-path mechanism validation and toxicity alteration. Chem Eng J. 2023; 474: 145837. https://doi.org/10.1016/j.cej.2023.145837

[32] Yu J, Deng W, Huang X, Zhao M, Li X, Zhang T*, et al.* Intramolecular generation of endogenous Cu(III) for selectively self-catalytic degradation of Cu(II)-EDTA from wastewater by UV/peroxymonosulfate. J Hazard Mater. 2024; 465: 133521. https://doi.org/10.1016/j.jhazmat.2024.133521

[33] Zhang L, Ju L, Li X, Guli A, Lyu C. CoOOH with a highly negative CB band for visible-light-driven photocatalytic degradation of refractory organic pollutants in peroxymonosulfate system: Enhanced performance and multi-path synergetic mechanisms. J Hazard Mater. 2023; 460: 132403. https://doi.org/10.1016/j.jhazmat.2023.132403

[34] Tang C, Wang C-C, Yi X-H, Chang M, Wang F, Li Y*, et al.* The enhanced photocatalytic peroxymonosulfate activation for 2, 4-dichlorophenoxyacetic acid degradation over Z-scheme PTCDA/MIL-88A(Fe) under visible light. Chem Eng J. 2024; 493: 152668. https://doi.org/10.1016/j.cej.2024.152668

[35] Liu Q, Cui K, Cui M, Liu X, Zhang Q. Co-modification of carbon and cyano defect in g-C_3N_4 for enhanced photocatalytic peroxymonosulfate activation: Combined experimental and theoretical analysis. Sep Purif Technol. 2023; 316: 123844. https://doi.org/10.1016/j.seppur.2023.123844

[36] Zhang L, Wang B, Yang W, Ju L, Fu Z, Zhao L*, et al.* CoOOH@COFs S−scheme heterojunction for efficient triclosan degradation in photocatalytic-peroxymonosulfate activation system: Enhanced interfacial electron transfer mechanism. Chin Chem Lett. 2025; (in press). https://doi.org/10.1016/j.cclet.2025.111142

[37] Jiang L, Xie S, Chen H, Yang J, Wang X, Li W*, et al.* Visible-light-promoted peroxymonosulfate activation for ACE degradation: Overlooked role of photogenerated hole. Appl Catal, B. 2025; 365: 124881. https://doi.org/10.1016/j.apcatb.2024.124881

[38] Deng Y, Liu J, Wu X, Zhou T, Huang M. Engineering Cu_2O@BN photocatalytic heterojunction for synchronous kinetic enhancement and reaction pathway regulation in peroxymonosulfate activation. J Environ Manage. 2025; 379: 124892. https://doi.org/10.1016/j.jenvman.2025.124892

[39] Yang Y, Meng W, Wang Y, Wang X, Wang J, Sun S-P, *et al.* Constructing 2D highly crystalline g-C_3N_4 supported 1D iron oxides in molten salts for enhanced photocatalytic peroxymonosulfate activation. Sep Purif Technol. 2025; 358: 130284. https://doi.org/10.1016/j.seppur.2024.130284

[40] Xu K, Cui K, Cui M, Liu X, Chen X, Tang X, *et al.* Electronic structure modulation of g-C_3N_4 by Hydroxyl-grafting for enhanced photocatalytic peroxymonosulfate Activation: Combined experimental and theoretical analysis. Sep Purif Technol. 2022; 294: 121246. https://doi.org/10.1016/j.seppur.2022.121246

[41] Bui T K, Nguyen T L, Van Pham V. Review of g-C_3N_4-based photocatalysts for Amoxicillin photocatalytic degradation. J Water Process Eng. 2024; 67: 106257. https://doi.org/10.1016/j.jwpe.2024.106257

[42] Bhattacharjee B, Mishra S R, Gadore V, Ahmaruzzaman M. Carbon-based Composites for Environmental Clean-up: Advances in Biochar, g-C_3N_4, Graphene Oxide and CNTs. J Taiwan Inst Chem Eng. 2025; 168: 105918. https://doi.org/10.1016/j.jtice.2024.105918

[43] Liu Q, Cui K, Cui M, Sun S, Li H. Sulfur and chloride co-doped g-C_3N_4 in photocatalytic peroxymonosulfate activation for enhanced acetaminophen removal: Combination of experiments and DFT calculations. J Environ Chem Eng. 2024; 12(3): 112857. https://doi.org/10.1016/j.jece.2024.112857

[44] Wu Z, Fan Z, Song P. Efficient degradation of Cu-Norfloxacin complexes in wastewater by electro-activated peroxymonosulfate coupled with electrocoagulation. J Water Process Eng. 2025; 70: 107140. https://doi.org/10.1016/j.jwpe.2025.107140

[45] Liu Y, Li Y, Li C, Asuna, Wang Z, Li F, *et al.* Electrochemically-induced metal–oxygen bond Cu(II)-SO_5^- on novel $CuBi_2O_4$ anode for efficient peroxymonosulfate activation. Chem Eng J. 2024; 495: 153378. https://doi.org/10.1016/j.cej.2024.153378

[46] Gao D, Wang H, Lu Q, Ye C, Cai J, Wang L. Enhanced PMS activation efficiency and SMX degradation performance via Fe(II)/Fe(III) cycling with efficient CCF@MoS_2@GA-Fe catalyst. Environ Res. 2025; 274: 121299. https://doi.org/10.1016/j.envres.2025.121299

[47] Zhang L, Li Z. Effect of dissolved oxygen on the peroxymonosulfate activation pathway in an electrochemical Co/P/CA cathode system. Chemosphere. 2024; 364: 143107. https://doi.org/10.1016/j.chemosphere.2024.143107

[48] Cai C, Jiang T, Peng H, Fu X, Nie C, Ao Z. Sustainable peroxymonosulfate activation by 1T/2H-MoS_2 cathode for enhanced removal of organic pollutants: Performance and nonradical activation mechanism based on surface Mo-peroxymonosulfate complexes. Chem Eng J. 2025; 518(15): 164474. https://doi.org/10.1016/j.cej.2025.164474

[49] Zhang L, Tao Y. Ecological regime shifts enhanced the contribution of microplastics to the burial of polycyclic aromatic hydrocarbons by sediments. Environ Pollut. 2023; 335: 122329. https://doi.org/10.1016/j.envpol.2023.122329

[50] Ma J, Lu J, Liu Y, Fan Z. Industrial potential of electro-oxidation and peroxymonosulfate coupling for efficient organic degradation in acidic dye wastewater. Process Saf Environ Protect. 2025; 194: 1572-1583. https://doi.org/10.1016/j.psep.2024.12.106

[51] Yu F, Guo Y, li H, Yang J. Activated persulfate by the synergistic electro-activation and bimetals cathode (MBC@CF) leads to highly efficient degradation of tetracycline. Sep Purif Technol. 2024; 335: 126204. https://doi.org/10.1016/j.seppur.2023.126204

[52] Wan H, Jin R, Tian Z, Qiu X, Zhai S, Niu J, *et al.* Electro-activation of peroxymonosulfate by novel Co_3O_4/sludge biochar cathode for sulfamethoxazole removal: cobalt-mediated synergistic effect and mechanism. Environ Res. 2025; 279: 121742. https://doi.org/10.1016/j.envres.2025.121742

[53] Zhao Y, Wang H, Ji J, Li X, Yuan X, Duan A, *et al.* Recycling of waste power lithium-ion batteries to prepare nickel/cobalt/manganese-containing catalysts with inter-valence cobalt/manganese synergistic effect for peroxymonosulfate activation. J Colloid Interface Sci. 2022; 626: 564-580. https://doi.org/10.1016/j.jcis.2022.06.112

[54] Gong M, Ren X, Chen J, Mo R, Yang S. Preparing of multi-metal spinel oxides for PMS activation from spent lithium-ion batteries: A non-closed-loop process. J Environ Chem Eng. 2025; 13(1): 115076. https://doi.org/10.1016/j.jece.2024.115076

[55] Hu Z, Su G, Long S, Zhang X, Zhang L, Chen Y, *et al.* Synthesis of X@DRHC (X=Co, Ni, Mn) catalyst from comprehensive utilization of waste rice husk and spent lithium-ion batteries for efficient peroxymonosulfate (PMS) activation. Environ Res. 2024; 245: 118078. https://doi.org/10.1016/j.envres.2023.118078

[56] Liu L, Zhu J, Liu Q, Wu Z. Mechanistic insights and performance evaluation of plasma-activated persulfate systems for the degradation of organic pollutants. Environ Res. 2025; 282: 122081. https://doi.org/10.1016/j.envres.2025.122081

[57] Duan Y, Dong B, Zhi X, Li Z, Wang P, Tan Y, *et al.* Degradation performance and mechanism of plasma-activated persulfate for environmental persistent pollutants. Chin J Chem Eng. 2025; 80: 155-65. https://doi.org/10.1016/j.cjche.2024.10.031

[58] Zhao X, Liu S, Tong Y, Sun L, Han Q, Feng L, *et al.* Comparative study on the activation of peroxymonosulfate and peroxydisulfate by Ar plasma-etching CNTs for sulfamethoxazole degradation: Efficiency and mechanisms. Chemosphere. 2024; 359: 142287. https://doi.org/10.1016/j.chemosphere.2024.142287

[59] Guo H, Pan S, Hu Z, Wang Y, Jiang W, Yang Y, *et al.* Persulfate activated by non-thermal plasma for organic pollutants degradation: A review. Chem Eng J. 2023; 470: 144094. https://doi.org/10.1016/j.cej.2023.144094

[60] Sang W, Bao H, Pang L, Cheng K, Li M, Zou L. Degradation of chlortetracycline in sludge by dielectric barrier discharge plasma coupled with peroxymonosulfate: Performance and mechanism. J Water Process Eng. 2024; 67: 106273. https://doi.org/10.1016/j.jwpe.2024.106273

[61] Hosseini R, Fattah-alhosseini A, Karbasi M, Giannakis S. Tailoring surface defects in Plasma Electrolytic Oxidation (PEO) treated 2-D black TiO_2: Post-treatment role, and intensification by peroxymonosulfate activation in visible light-driven photocatalysis. Appl Catal, B. 2024; 340: 123197. https://doi.org/10.1016/j.apcatb.2023.123197

[62] Liu S, Yin S, Zhang Z, Feng L, Liu Y, Zhang L. Regulation of defects and nitrogen species on carbon nanotube by plasma-etching for peroxymonosulfate activation: Inducing non-radical/radical oxidation of organic contaminants. J Hazard Mater. 2023; 441: 129905. https://doi.org/10.1016/j.jhazmat.2022.129905

[63] Liu S, Zhang Z, Lu R, Mao Y, Ge H, Liu C*, et al.* O_2 plasma-modified carbon nanotube for sulfamethoxazole degradation via peroxymonosulfate activation: Synergism of radical and non-radical pathways boosting water decontamination and detoxification. Chemosphere. 2023; 344: 140214. https://doi.org/10.1016/j.chemosphere.2023.140214

[64] Sun C, Wang H, Jiang T, Zhao X, Yao M, Wang X*, et al.* Surface defect and carbonyl engineering of CNTs via oxygen-plasma etching: Oriented production of singlet oxygen from peroxymonosulfate activation. Sep Purif Technol. 2024; 337: 126454. https://doi.org/10.1016/j.seppur.2024.126454

[65] Chen Y, Sun X, Zheng L, Liu Y, Zhao Y, Huang S*, et al.* Synergistic catalysis induced by a multi-component system constructed by DBD plasma combined with α-Fe_2O_3/$FeVO_4$/HCP and peroxymonosulfate for gatifloxacin removal. Chemosphere. 2023; 332: 138838. https://doi.org/10.1016/j.chemosphere.2023.138838

[66] Lou J, Wang X, An J. Dielectric barrier discharge plasma in-situ microbubble aeration with peroxymonosulfate for levofloxacin degradation: Microbubble superior performance and pH-dependent mechanism. Sep Purif Technol. 2025; 355: 129626. https://doi.org/10.1016/j.seppur.2024.129626

[67] Jia M, Pei X, Cheng J, Tian D, Yang J, Sang L*, et al.* An excellent defluorination rate of PFOA achieved by a DBD-peroxymonosulfate system. J Water Process Eng. 2025; 76: 108215. https://doi.org/10.1016/j.jwpe.2025.108215

[68] Lou J, Lu G, Wei Y, Zhang Y, An J, Jia M*, et al.* Enhanced degradation of residual potassium ethyl xanthate in mineral separation wastewater by dielectric barrier discharge plasma and peroxymonosulfate. Sep Purif Technol. 2022; 282: 119955. https://doi.org/10.1016/j.seppur.2021.119955

[69] You C-S, Jung S-C. Decomposition of the antibiotic sulfamethoxazole by the liquid-phase plasma process enhanced by peroxymonosulfate. J Ind Eng Chem. 2024; 131: 422-31. https://doi.org/10.1016/j.jiec.2023.10.045

[70] Liu S, Kang Y. Synergistic oxidation induced by underwater bubbling plasma and diatomite-$CoFe_2O_4$ activated peroxymonosulfate for the degradation of ciprofloxacin hydrochloride. Environ Pollut. 2024; 348: 123891. https://doi.org/10.1016/j.envpol.2024.123891

[71] Hua W, Kang Y, Liu S. Synergistic removal of aqueous ciprofloxacin hydrochloride by water surface plasma coupled with peroxymonosulfate activation. Sep Purif Technol. 2022; 303: 122301. https://doi.org/10.1016/j.seppur.2022.122301

[72] Hongchao L, Zihao Z, Jieshu Q, Bingcai P. Are Free Radicals the Primary Reactive Species in Co(II)-Mediated Activation of Peroxymonosulfate? New Evidence for the Role of the Co(II)-Peroxymonosulfate Complex. Environ Sci Technol. 2021; 55(9): 6397-6406. http://dx.doi.org/10.1021/ACS.EST.1C02015

[73] Hongyu D, Qinghua X, Lushi L, Yang L, Shuchang W, Cong L*, et al.* Degradation of Organic Contaminants in the Fe(II)/Peroxymonosulfate Process under Acidic Conditions: The Overlooked Rapid Oxidation Stage. Environ Sci Technol. 2021; 55(22): 15390-9. http://dx.doi.org/10.1021/ACS.EST.1C04563

[74] Yang B, Ma Q, Hao J, Sun X. Peroxymonosulfate Activation by Palladium(II) for Pollutants Degradation: A Study on Reaction Mechanism and Molecular Structural Characteristics. Int J Environ Res Public Health. 2022; 19(20): 13036. http://dx.doi.org/10.3390/IJERPH192013036

[75] Li J, Ni Z, Gao Q, Yang X, Fang Y, Qiu R*, et al.* Core-shell structured cobalt–nickel bimetallic sulfide with dual redox cycles to activate peroxymonosulfate for glyphosate removal. Chem Eng J. 2023; 453: 139972. https://doi.org/10.1016/j.cej.2022.139972

[76] Wang X, Xia L, Cheng H, Li K, Feng W, Dai X*, et al.* Ultrasound-mediated Cu^{2+}/Cu^{+} redox cycling activates peroxymonosulfate for oxygen-independent reactive X species (X = O/S) therapy. Nano Today. 2024; 55: 102180. https://doi.org/10.1016/j.nantod.2024.102180

[77] Pan M, Hamid Y, Czech B, He Z, Yang X. Hyperaccumulator biochar prepared via hydrothermal pretreatment for azo dye degradation: Peroxymonosulfate activation and life cycle assessment. J Environ Chem Eng. 2025; 13(3): 116796. https://doi.org/10.1016/j.jece.2025.116796

[78] Bu Z, Hou M, Li Z, Dong Z, Zeng L, Zhang P*, et al.* Fe^{3+}/Fe^{2+} cycle promoted peroxymonosulfate activation with addition of boron for sulfamethazine degradation: Efficiency and the role of boron. Sep Purif Technol. 2022; 298: 121596. https://doi.org/10.1016/j.seppur.2022.121596

[79] Li G, Cheng Y, Chen Y, Liu Z, Ma J, Xie P. Accelerated vanadium (IV)/(V) redox cycle and hydroxyl radical generation by hydroxylamine in peroxymonosulfate activation: from synthetic vanadium oxides to natural minerals. Chem Eng J. 2025; 518: 164821. https://doi.org/10.1016/j.cej.2025.164821

[80] Liu H, An L, Gao Z, Duan Z, Luo B, Sun Y*, et al.* The removal of antibiotic resistance bacteria and genes and inhibition of RP4 plasmid-mediated conjugative transfer by citric acid chelated Fe(II) catalyzing peroxymonosulfate systems: Performance and mechanisms. Chem Eng J. 2024; 499: 156297. https://doi.org/10.1016/j.cej.2024.156297

[81] Ma MD, Zhao YC, Zhu L, Wang WP, Kang YL, An LH. Research Progress on Characteristics of Human Microplastic Pollution and Health Risks. Environ Sci. 2024; 45(1): 459-69. 10.13227/J.HJKX.202212185

[82] Liu H, Zhao J, Wang Y, Wu Y, Dong W, Nie M*, et al.* Enhancement of peroxymonosulfate activation by sinapic acid accelerating Fe(III)/Fe(II) cycle. Chem Eng J. 2022; 446: 137177. https://doi.org/10.1016/j.cej.2022.137177

[83] Wang S, Xia J, Zha Y, Zhu J, Wang Y, Huang R*, et al.* Ceramic catalytic membrane with low metal ion leaching for bisphenol A removal via peroxymonosulfate activation. Chem Eng Sci. 2025; 301: 120698. https://doi.org/10.1016/j.ces.2024.120698

[84] Gao S, Han X, Zhang Y, Zhang L, Tian Z, Xiong Y, *et al.* Mn/Ce nanoparticles doped carbon nanotubes with enhanced redox cycles for efficient and stable peroxymonosulfate activation. Appl Surf Sci. 2025; 706: 163549. https://doi.org/10.1016/j.apsusc.2025.163549

[85] Sui C, Nie Z, Liu H, Boczkaj G, Liu W, Kong L, *et al.* Singlet oxygen-dominated peroxymonosulfate activation by layered crednerite for organic pollutants degradation in high salinity wastewater. J Environ Sci. 2024; 135: 86-96. https://doi.org/10.1016/j.jes.2023.01.010

[86] Shen Y, Martín de Vidales M J, Gorni G, Sampaio M J, Silva A M T, Lado Ribeiro A R, *et al.* Composition-dependent PMS activation in $Sr_xLa_{2-x}CoO_{4\pm\delta}$ perovskite-derivatives: From radical to strengthen the electron-transfer pathway. Appl Catal, B. 2024; 357: 124291. https://doi.org/10.1016/j.apcatb.2024.124291

[87] Wang Q, Yu W, Xu W, Li Z, Xia X, Xu Y. Trace copper doped $LaMnO_3$ perovskite for PMS activation via electron transfer process towards pollutant elimination. J Water Process Eng. 2025; 72: 107486. https://doi.org/10.1016/j.jwpe.2025.107486

[88] Zhang X, Zhang W, Li J, Wang T, Miao H, Fan Q, *et al.* Nanosized Co-Fe spinel quantum dots anchored on activated carbon for enhanced VOCs mineralization via PMS-based AOPs coupled with wet scrubber. Sep Purif Technol. 2024; 328: 125135. https://doi.org/10.1016/j.seppur.2023.125135

[89] Han X, Li G, Su W, Xu X, Yu M, Wu G, *et al.* Cu-based composite materials derived from MOFs for visible light PMS activation in tetracycline removal. Colloids Surf, A. 2024; 702: 135147. https://doi.org/10.1016/j.colsurfa.2024.135147

[90] Hong Y, Huang Z, Xu J, Xue Y, Feng H, Zhang T, *et al.* Surging efficient PMS activation through a COF-MOF dual immobilized catalytic platform: Synergy of enhanced electron transfer and adsorption-PMS activation. Sep Purif Technol. 2024; 345: 127376. https://doi.org/10.1016/j.seppur.2024.127376

[91] Pan J, Wang Z, Luo J, Fan L, Li X, Wang C, *et al.* Uncovering the high-activity origin of sulfur doping in Co_3O_4 for organic pollutant degradation via peroxymonosulfate activation. Chem Eng J. 2025; 515: 163760. https://doi.org/10.1016/j.cej.2025.163760

[92] Yang Z, Zheng G, Wang X, Wen K, Chen X, Zhang J. Ferroelectric $Bi_2Fe_4O_9$ for efficient peroxymonosulfate activation: The overlooked role of spontaneous polarization. Sep Purif Technol. 2025; 374: 133787. https://doi.org/10.1016/j.seppur.2025.133787

[93] Bian H, OuYang Z, Zhang X, Wang J. Efficient activation of peroxymonosulfate by CoCuAl-LDH nanosheets for the degradation of RhB. J Solid State Chem. 2025; 349: 125414. https://doi.org/10.1016/j.jssc.2025.125414

[94] Wang Z, Gao L, Chen X, Jin H, Wei H, Ma L, *et al.* Hollow layered double hydroxide nanoreactor activated peroxymonosulfate to efficiently degrade dye wastewater. J Colloid Interface Sci. 2025; 689: 137205. https://doi.org/10.1016/j.jcis.2025.02.213

[95] Li T, Sun W, Zhang J, Liu S, Chen H, Qiu Z, *et al.* Co_3O_4 confined in activated carbon-supported Mg/Al-LDH for μM peroxymonosulfate activation with minute-level antibiotics degradation. Chem Eng J. 2025; 516: 163872. https://doi.org/10.1016/j.cej.2025.163872

[96] Li W, Kong L, Wang Z, Han Z, Zhang B, Shi M, *et al.* Electronic structure reconstruction of Fe-Mn diatomic pair for disentangling activity-stability tradeoff in Fenton-like reactions. Appl Catal, B. 2025; 365: 124920. https://doi.org/10.1016/j.apcatb.2024.124920

[97] Li H, Li N, Xu C, Huang J, Du J, Li F, *et al.* Highly efficient activation of peroxymonosulfate by MOF derived CoS_2@C for degradation of ciprofloxacin. Sep Purif Technol. 2025; 352: 128275. https://doi.org/10.1016/j.seppur.2024.128275

[98] Liu Y, Liu H, Li Z, Qin H, Di S, Chen P, *et al.* N-doped CuFe-MOF-919 derivatives in activation of peroxymonosulfate for enhanced degradation of organic pollutants: $^1O_2$ dominated non-radical pathway. Sep Purif Technol. 2024; 345: 127324. https://doi.org/10.1016/j.seppur.2024.127324

[99] Wang H, Dai Y, Wang Y, Yin L. One-pot solvothermal synthesis of Cu–Fe-MOF for efficiently activating peroxymonosulfate to degrade organic pollutants in water:Effect of electron shuttle. Chemosphere. 2024; 352: 141333. https://doi.org/10.1016/j.chemosphere.2024.141333

[100] Peng X, Li J, Liu S, Zeng P, Shan M. Bimetallic FeCo-MOF as peroxymonosulfate activator for efficient degradation of sulfamethoxazole: Performance and mechanism. Mol Catal. 2025; 572: 114751. https://doi.org/10.1016/j.mcat.2024.114751

[101] Guo S, Li J, Wang Y, Sun D, Ma H, Hao J, *et al.* Polydopamine-modified bimetallic metal organic frameworks (MOFs) for peroxymonosulfate activation to efficient degradation of tetracycline hydrochloride in wastewater. Colloids Surf, A. 2024; 689: 133721. https://doi.org/10.1016/j.colsurfa.2024.133721

[102] Wang H, Zang J, Zhang Y, Zhang J, Pu Y, Long Y, *et al.* Cobalt boride derived from metal-organic framework as highly efficient catalyst for tetracycline degradation with peroxymonosulfate activation. J Environ Chem Eng. 2025; 13: 117580. https://doi.org/10.1016/j.jece.2025.117580

[103] Zhang C, Chen L, Luo H, Weng H, Qin F, Qin D, *et al.* Selective micropollutants removal in wastewaters by non-radical activation of peroxymonosulfate: Multiparameter analysis of electron-donating capacity. Appl Catal, B. 2025; 362: 124695. https://doi.org/10.1016/j.apcatb.2024.124695

[104] Yang Y, Yang B, Gao X, Dang X, Jin Z, Zhang X. MOF-on-MOF composite material derived from ZIF-67 precursor activated by peroxymonosulfate for the removal of metronidazole. J Water Process Eng. 2025; 72: 107467. https://doi.org/10.1016/j.jwpe.2025.107467

[105] Li X, Fu X, Wu J, Fu X, Huang J, Chen Y. MOF derived bimetallic-nanoreactor as peroxymonosulfate activator for highly efficient levofloxacin degradation: Performance and mechanism. Chem Eng J. 2025; 515: 163948. https://doi.org/10.1016/j.cej.2025.163948

[106] Di L, Wang T, Lu Q, Lu J, Zhang Y, Zhou Y, *et al.* Efficient PMS activation toward degradation of bisphenol A by metal-free nitrogen-doped hollow carbon spheres. Sep Purif Technol. 2024; 339: 126740. https://doi.org/10.1016/j.seppur.2024.126740

[107] Gao Y, Zhao H, Liu M, Wang Y, Zhang Y, Zhai L, *et al.* Construction of photothermal hybrid with surface-polarized carbon nanotube twined oxygen-vacancy engineered cuprous oxide for improved PMS activation and water purification. Mol Catal. 2025; 578: 114994. https://doi.org/10.1016/j.mcat.2025.114994

[108] Tao F, Chen H, Wang H, Huang H, Dong A, Zheng M, *et al.* Efficient degradation of organic pollutants using carbon coil aerogels from waste tea as peroxymonosulfate activators. J Water Process Eng. 2025; 70: 107064. https://doi.org/10.1016/j.jwpe.2025.107064

[109] Su B, Zhang W, Sun F, Quan X. Hybrid peroxymonosulfate/activated carbon fiber-sequencing batch reactor system for efficient treatment of coking wastewater: Establishment and influential factors. Bioresour Technol. 2024; 405: 130907. https://doi.org/10.1016/j.biortech.2024.130907

[110] Huang X, Liu C, Zhang Z, Vasanthakumar V, Ai H, Xu L, *et al.* Stable Cu-Co/C carbon-based composites for efficiency catalytic degradation of Orange II by PMS: Effect factors, application potential analysis, and mechanism. J Ind Eng Chem. 2023; 126: 307-16. https://doi.org/10.1016/j.jiec.2023.06.021

[111] Li M, Zhang W, Lin L, Gong Z, Li B, Sun F, *et al.* Facet regulation of nanocrystal cobalt@nitrogen-carbon catalyst for boosting PMS activation towards carbamazepine degradation. Sep Purif Technol. 2025; 363: 132169. https://doi.org/10.1016/j.seppur.2025.132169

[112] Li F, Yuan C, Niu Y, Sheng J, Wang X, Shi Y, *et al.* Cobalt/iron bimetallic oxide coated with graphitized nitrogen-doped carbon (Fe_2O_3-CoO@NC) derived from cobalt/iron solid complex as peroxymonosulfate (PMS) activator for efficient bensulfuron-methyl degradation. Environ Res. 2024; 263: 120249. https://doi.org/10.1016/j.envres.2024.120249

[113] Yang J, Zhao H, Qiu S, Xiong F, Fu B, Zhang F, *et al.* Oxidative degradation of anionic dyes in wastewater by magnetic lignin micro-nano spheres catalyzed peroxymonosulfate. Int J Biol Macromol. 2024; 282: 137390. https://doi.org/10.1016/j.ijbiomac.2024.137390

[114] Yu C, Gu L, Wu Z, Chen K, Wu Y, Zhang L, *et al.* N-coordinated iron sites dispersed in porous carbon frameworks to activate peroxymonosulfate for efficient sulfisoxazole degradation and real hospital wastewater decontamination. J Hazard Mater. 2024; 480: 136149. https://doi.org/10.1016/j.jhazmat.2024.136149

[115] Yuexing W, Bin F, Junmei G, Jiansheng Z, Yuhong Q, Chong H, *et al.* Co_3O_4 coated carbon fiber activates PMS to degrade phenolic pollutants via $^1O_2$ dominated non-radical pathway: Role of dual reaction center. J Environ Chem Eng. 2024; 12(5): 113921. https://doi.org/10.1016/j.jece.2024.113921

[116] Guo X, Yang N, Qi J, Li X, Guo D. Dopping-elements electronegativity-guided electronic modulation of N, P doped carbon coated CoFeP: Dual-functional contaminant degradation via electrooxidation and PMS (Peroxymonosulfate) activation. Sep Purif Technol. 2025; 373: 133544. https://doi.org/10.1016/j.seppur.2025.133544

[117] Liu S, Wang B, Huang Y, Xu X, Kan Y, Shang Y. Comparison between endogenous and exogenous nitrogen of nitrogen-doped carbon catalyst in the process of activating PMS. J Taiwan Inst Chem Eng. 2024; 165: 105793. https://doi.org/10.1016/j.jtice.2024.105793

[118] Chen X, Wang D, Tan K, Dong L. In situ self-assembly green synthesis of P-doped tubular carbon nitride for photocatalytic activation of PMS to rapidly degrade organic pollutants. J Environ Sci. 2025 (in press). https://doi.org/10.1016/j.jes.2025.04.019

[119] Zhi K, Liu D, Xu J, Li Z, Li S, Luo L, *et al.* N-doped graphene loaded with Ru sites as PMS activators for SMX degradation via non-radical pathway: efficiency, selectivity and mechanism. Chem Eng J. 2025; 512: 162230. https://doi.org/10.1016/j.cej.2025.162230

[120] Hou L, Zang J, Liu S, You P, Fan G. Nitrogen-mediated engineering cobalt phosphide sites for enhanced peroxymonosulfate activation towards organic wastewater purification. Environ Res. 2025; 277: 121551. https://doi.org/10.1016/j.envres.2025.121551

[121] Andoh C N, Attiogbe F, Bonsu Ackerson N O, Antwi M, Adu-Boahen K. Fourier Transform Infrared Spectroscopy: An analytical technique for microplastic identification and quantification. Infrared Phys Technol. 2024; 136: 105070. 10.1016/j.infrared.2023.105070

[122] Le V-A, Nguyen H T, Wang Y-F, You S-J. Effective integration of peroxymonosulfate activation and photocatalysis by MnO_2@CeO_2 catalyst for enhanced membrane antifouling performance. Sep Purif Technol. 2025; 376: 133877. https://doi.org/10.1016/j.seppur.2025.133877

[123] Pan B, Chen W, Zhou L, Lai X, Qin J, Wang C. $CoFe_2O_4$/carbon nitride Z-scheme heterojunction photocatalytic PMS activation for efficient tetracycline degradation: Accelerated electron transfer. Process Saf Environ Protect. 2024; 191: 2522-32. https://doi.org/10.1016/j.psep.2024.09.120

[124] Zhou M, Huang X, Zhang Y, Zhou N, Deng J, Zeng Y, *et al.* Synergistic combination of Mn/Fe bimetal-doped carbon nitride and peroxymonosulfate for efficient photocatalytic degradation of antibiotics. J Environ Chem Eng. 2024; 12(5): 113730. https://doi.org/10.1016/j.jece.2024.113730

[125] Wei LW, Liu SH, Nguyen VC, Zheng MW, Wang HP. Visible-light driven O_2-to-H_2O_2 synchronized activation of peroxymonosulfate in Z-scheme photocatalytic fuel cell for wastewater purification with power generation. Appl Catal, B. 2025; 361: 124594. https://doi.org/10.1016/j.apcatb.2024.124594

[126] Sun Y, Xia L, Wang Y, Yao W, Wu Q, Min Y, *et al.* Efficient rifampicin degradation and simultaneous energy recovery in photocatalytic fuel cell based on the enhanced PMS and H_2O_2 synergistic activation on sulfur-doped CuMnO/carbon felt cathode. Sep Purif Technol. 2023; 326: 124831. https://doi.org/10.1016/j.seppur.2023.124831

[127] Zhang J, Chang L, Zhu X, Yao J, Bai A, Wang J, *et al.* Large-scale and green synthesis of flower-like MgO from waste magnesite activated PMS for oxidation of doxycycline. Appl Surf Sci. 2025; 685: 161993. https://doi.org/10.1016/j.apsusc.2024.161993

[128] Guo L, Chen S, Jiang Y, Ding Q, Yang Y, Zhi J, *et al.* N, S co-doped porous carbon derived from waste medical masks to support $LaFe_xCo_{1-x}O_3$ as highly effective peroxymonosulfate catalysts for degradation of tetracycline. J Environ Chem Eng. 2024; 12(5): 113655. https://doi.org/10.1016/j.jece.2024.113655

[129] Zhang W, Liu J, Liu S, Huang E, Ren S, Gong L. Hollow ZIF-67-loaded sandy sediment for enhanced solar-driven water evaporation and PMS-activated pollutant degradation. Chem Eng J. 2025; 506: 159900. https://doi.org/10.1016/j.cej.2025.159900

[130] Zhou J, Zhao H, Zhang Y, Zhu H, Cai Y, Wang Y, *et al.* Solar-driven PMS activation over Ag/Halloysite nanotubes onto floatable integrated device for pollutant degradation and coupled interfacial water evaporation. Mol Catal. 2025; 583: 115248. https://doi.org/10.1016/j.mcat.2025.115248

[131] Lin Y, Zhang Y, Wang Y, Lv Y, Yang L, Chen Z, *et al.* Efficient degradation and mineralization of polyethylene terephthalate microplastics by the synergy of sulfate and hydroxyl radicals in a heterogeneous electro-Fenton-activated persulfate oxidation system. J Hazard Mater. 2024; 478: 135635. https://doi.org/10.1016/j.jhazmat.2024.135635

[132] Yu M, Chen M, Yang C, Niu J, Zhang J, Mu S, *et al.* Sustainable Fe(II) oxidation/reduction and release/recovery dual cycle in a multi-chamber Fe(III)/Peroxymonosulfate electrochemical system: Application, mechanism, and optimization. Chem Eng J. 2025; 512: 162601. https://doi.org/10.1016/j.cej.2025.162601

[133] Zou L, Hu Y, Lv Y, Liu Y, Ye X, Lin C, *et al.* Non-free radical regulation mechanism based on pH in the peroxymonosulfate activation process mediated by single-atom Co catalyst for the specific rapid degradation of emerging pollutants. J Colloid Interface Sci. 2025; 687: 617-29. https://doi.org/10.1016/j.jcis.2025.02.110

[134] Li J, Huang W, Yang L, Gou G, Zhou C, Li L, *et al.* Novel Ag_3PO_4 modified tubular carbon nitride with visible-light-driven peroxymonosulfate activation: A wide pH tolerance and reaction mechanism. Chem Eng J. 2022; 432: 133588. https://doi.org/10.1016/j.cej.2021.133588

[135] Ahn Y-Y, Kim J, Jeon J, Kim K. Freezing-enhanced degradation of azo dyes in the chloride-peroxymonosulfate system. Chemosphere. 2024; 359: 142261. https://doi.org/10.1016/j.chemosphere.2024.142261

[136] Le N T H, Ju J, Kim B, Kim M S, Lee C, Kim S, *et al.* Freezing-enhanced non-radical oxidation of organic pollutants by peroxymonosulfate. Chem Eng J. 2020; 388: 124226. https://doi.org/10.1016/j.cej.2020.124226

[137] Tang Y, Wang L, Fu Y, Wang Z. Temperature-regulated non-radical to radical oxidation of organic pollutants by peroxymonosulfate: A tale of ice and fire. J Water Process Eng. 2025; 72: 107608. https://doi.org/10.1016/j.jwpe.2025.107608

[138] Guo X, Du B, Yan W, Wu Y, Feng J, Zhu Y. Efficient activation of peroxymonosulfate by sulfur vacancies engineered $NiCo_2S_4$ spheres for norfloxacin degradation. Environ Res. 2025; 283: 122129. https://doi.org/10.1016/j.envres.2025.122129

[139] Yu Z, Wang S, Chen Z, Yan X, Wang J, Jiang F, *et al.* Treating waste with waste: Enhancing performance of titanium gypsum by co-calcination of waste sludge for sulfamethoxazole degradation using peroxymonosulfate activation. J Water Process Eng. 2025; 74: 107880. https://doi.org/10.1016/j.jwpe.2025.107880

[140] Wu J, Wen Y, Leng Z, Zhang S, Li S, Zhou Z, *et al.* Enhanced atrazine degradation in water by N, P co-doped biochar based on peroxymonosulfate: Performance, mechanism and phytotoxicity reduction. J Environ Chem Eng. 2025; 13(2): 116002. https://doi.org/10.1016/j.jece.2025.116002

[141] Fu D, Zhao Z, Yan P, Chen Z, Zuo J. Oxygen-vacancy-rich N-doped $NiFe_2O_4$ activates peroxymonosulfate for efficient water purification. Sep Purif Technol. 2025; 376: 134061. https://doi.org/10.1016/j.seppur.2025.134061

[142] Wang Y, Chen Y, Li Y, Zhang I Y, Huang R. Application of Fe-ethylene diamine tetraacetic acid complex to enhance the electrocatalytic activation of peroxymonosulfate under neutral pH condition for removal of refractory naphthenic acids. Sep Purif Technol. 2024; 341: 126862. https://doi.org/10.1016/j.seppur.2024.126862

[143] Liu S, Bu W, Hou X, Lu S, Zhou C, Song X, *et al.* Insights into the enhanced removal of ciprofloxacin by $Ni_1Mn_1Fe_1$-LDO activated peroxymonosulfate: Mechanism and application for antibiotic wastewater. Process Saf Environ Protect. 2025; 196: 106853. https://doi.org/10.1016/j.psep.2025.106853

[144] Li H, Wu J, Ren A, Qu Y, Zong X, Gong Y, *et al.* Shaddock peels biochar doping with Fe-Co bimetal for peroxymonosulfate activation on the degradation of tetracycline: The influence of HCO_3^- and PO_4^{3-}. Environ Res. 2025; 275: 121411. https://doi.org/10.1016/j.envres.2025.121411

[145] Peng X, Zhou M, Yuan Q, Fan M, Zhu J, Gao N, *et al.* Degradation of organic pollutants in water by inactive and chloride salt-activated peroxymonosulfate (PMS): performance, kinetics, mechanisms and practical applications. J Ind Eng Chem. 2025 (in press). https://doi.org/10.1016/j.jiec.2025.06.008

[146] Saha P, Zhou C, Moradi M, Rijnaarts HM, Bruning H. Heat-activated peroxydisulfate and peroxymonosulfate-mediated degradation of benzotriazole: Effects of chloride on kinetics, pathways and transformation product toxicity. Chem Eng J Adv. 2023; 14: 100472. https://doi.org/10.1016/j.ceja.2023.100472

[147] Huang Y, Zhang S, Chen L, Kou X, Hou Y, Wu Z, *et al.* Removal of ammonia nitrogen in maricultural wastewater with Cl^-/peroxymonosulfate process: Performances and mechanism. J Environ Chem Eng. 2025; 13(2): 115549. https://doi.org/10.1016/j.jece.2025.115549

[148] Liu X, Wang Y, Crittenden J, Su Q, Mo H. Enhanced treatment of high chloride organic wastewater under lower peroxymonosulfate consumption: A pathway for the formation of Fe(IV)=O excited by chloride ions. Appl Catal, B. 2024; 359: 124471. https://doi.org/10.1016/j.apcatb.2024.124471

[149] Bao J, Wei Y, Lu Z, Yan S, Li H, Fang M, *et al.* Halogen ions enhanced peroxymonosulfate oxidation of emerging organic contaminants in municipal wastewater: Effect of environmental temperature. Chem Eng J. 2025; 504: 158290. https://doi.org/10.1016/j.cej.2024.158290

[150] Song Z, Zhang Y, He P, Liu X, Ren N, Chen Y. Feasibility of phenolic contaminant removal from high-saline wastewater by chloride-mediated activation of peroxymonosulfate (PMS) and peracetic acid (PAA). Sep Purif Technol. 2024; 341: 126856. https://doi.org/10.1016/j.seppur.2024.126856

[151] Song S, Liu W, Wang M, Xue J, Yao M. Beneficial utilization of ball-milled carbon sand to activate peroxymonosulfate oxidation: Quantitation of ROS using probe-based kinetic models and mechanism insights. J Environ Manage. 2024; 370: 122568. https://doi.org/10.1016/j.jenvman.2024.122568

[152] Gao L, Guo Y, Huang J, Wang B, Deng S, Yu G*, et al.* Simulating micropollutant abatement during cobalt mediated peroxymonosulfate process by probe-based kinetic models. Chem Eng J. 2022; 441: 135970. https://doi.org/10.1016/j.cej.2022.135970

[153] Sun Y, Ma C, Wu D, Liu X, Li N, Fan X*, et al.* Coating $CoFe_2O_4$ shell on Fe particles to increase the utilization efficiencies of Fe and peroxymonosulfate for low-cost Fenton-like reactions. Water Res. 2023; 244: 120542. https://doi.org/10.1016/j.watres.2023.120542

[154] Xu X, Peng C, Shao X, Gong K, Zhao X, Xie W*, et al.* Unveiling the impacts of biodegradable microplastics on cadmium toxicity, translocation, transformation, and metabolome in lettuce. Sci Total Environ. 2024; 957: 177669. 10.1016/j.scitotenv.2024.177669

[155] Yuan T, Zhao Y, An Y, Li X. Unraveling the contribution of Co(IV) and free radicals in Co^{2+}-activated Peroxymonosulfate process: Reaction mechanism, degradation pathway, and DFT calculation. Emerging Contam. 2024; 10(1): 100273. https://doi.org/10.1016/j.emcon.2023.100273

[156] Zhang Y, He R, Sun Y, Zhao J, Zhang X, Wang J*, et al.* Influence of microplastics and environmentally persistent free radicals on the ability of biochar components to promote degradation of antibiotics by activated peroxymonosulfate. Environ Pollut. 2024; 349: 123827. https://doi.org/10.1016/j.envpol.2024.123827

[157] Zhou X, Li Z, Shi Y, Miao Y, Liu Y, Yin R*, et al.* Piezoelectric field-modulated peroxymonosulfate nonradical oxidation of bisphenol A via Bio-MOF-1: The dominant contribution of singlet oxygen. Chem Eng J. 2024; 492: 152368. https://doi.org/10.1016/j.cej.2024.152368

[158] Li S, Zou J, Wu J, Lin J, Wu Z, Tang C*, et al.* Overlooked role of protocatechuic acid in enhancing the selective elimination of sulfonamide antibiotics in Fe(III)/peroxymonosulfate process under actually neutral pH conditions. Chem Eng J. 2024; 497: 154581. https://doi.org/10.1016/j.cej.2024.154581

[159] Shi L, Li Y, Dong H, Sun J, Xia C, Cai L*, et al.* Heterostructural Cu_2S@CuO nanoarrays enable peroxymonosulfate activation for sulfamethoxazole degradation through non-free radical pathways. Desalin. 2025; 600: 118527. https://doi.org/10.1016/j.desal.2025.118527

[160] Qin X, Li H, Yu Y, Yang Y, Wang K, Ma T*, et al.* Ornidazole degradation based on peroxymonosulfate activation induced by oxygen vacancies (OV)-enriched Cu-Co-TiO_2: Coexistence of free-radical and non-radical pathways. Process Saf Environ Protect. 2024; 192: 1008-25. https://doi.org/10.1016/j.psep.2024.10.099